# NUMERICAL EXPERIMENTS ON THE COMPUTATION OF GROUND SURFACE TEMPERATURE IN AN ATMOSPHERIC CIRCULATION MODEL

Chandrakant M. Bhumralkar

RAND Corporation

Prepared for:

Defense Advanced Research Projects Agency

May 1974

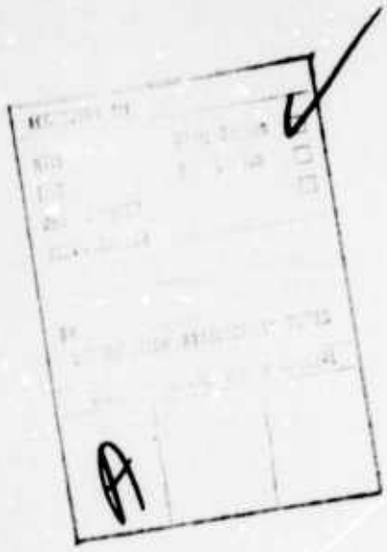

The research described in this Report was sponsored by the Defense Advanced Research Projects Agency under contract No. DAHC15-73-C-0181. Reports of The Rand Corporation do not necessarily reflect the opinions or policies of the sponsors of Rand research.

UNCLASSIFIED
SECURITY CLASSIFICATION OF THIS PAGE (When Data Entered)

AD-783922

# REPORT DOCUMENTATION PAGE

READ INSTRUCTIONS BEFORE COMPLETING FORM

| | |
|---|---|
| 1. REPORT NUMBER: R-1511-ARPA | 2. GOVT ACCESSION NO. |
| 3. RECIPIENT'S CATALOG NUMBER | |
| 4. TITLE (and Subtitle): Numerical Experiments on the Computation of Ground Surface Temperature in an Atmospheric Circulation Model | 5. TYPE OF REPORT & PERIOD COVERED: Interim |
| 6. PERFORMING ORG. REPORT NUMBER | |
| 7. AUTHOR(s): Chandrakant M. Bhumralkar | 8. CONTRACT OR GRANT NUMBER(s): DAHC15-73-C-0181 |
| 9. PERFORMING ORGANIZATION NAME AND ADDRESS: The Rand Corporation, 1700 Main Street, Santa Monica, Ca. 90406 | 10. PROGRAM ELEMENT, PROJECT, TASK AREA & WORK UNIT NUMBERS |
| 11. CONTROLLING OFFICE NAME AND ADDRESS: Defense Advanced Research Projects Agency, Arlington, VA | 12. REPORT DATE: May 1974<br>13. NUMBER OF PAGES: 62 |
| 14. MONITORING AGENCY NAME & ADDRESS (if different from Controlling Office) | 15. SECURITY CLASS. (of this report): UNCLASSIFIED<br>15a. DECLASSIFICATION DOWNGRADING SCHEDULE |

16. DISTRIBUTION STATEMENT (of this Report)

Approved for Public Release; Distribution Unlimited

17. DISTRIBUTION STATEMENT (of the abstract entered in Block 20, if different from Report)

18. SUPPLEMENTARY NOTES

19. KEY WORDS (Continue on reverse side if necessary and identify by block number)

Climatology
Climate Simulation
Weather Modeling

20. ABSTRACT (Continue on reverse side if necessary and identify by block number)

see reverse side



DD FORM 1 JAN 73 1473 EDITION OF 1 NOV 65 IS OBSOLETE

UNCLASSIFIED
SECURITY CLASSIFICATION OF THIS PAGE (When Data Entered)

Integration of the Rand two-level general circulation model to compute the ground (bare land only) surface temperature by solving (1) the interface heat balance equation *without* soil heat flux, (2) the interface heat balance equation *with* soil heat flux included, and (3) a prognostic equation which includes the heat capacity of the soil as well as an explicit soil heat flux formulation. The intergrations were performed for 48 hours for the month of January. A comparison of results shows that the most realistic distribution of the ground surface temperature with respect to the amplitude, diurnal range, and phase relationship between ground temperature, solar radiation, and soil heat flux is obtained by the method which solves a prognostic equation including the soil heat flux as well as the soil heat capacity.

ARPA ORDER NO.: 189-1
3P10 Distributed Information Systems

R-1511-ARPA
May 1974

# Numerical Experiments on the Computation of Ground Surface Temperature in an Atmospheric Circulation Model

C. M. Bhumralkar

A Report prepared for

DEFENSE ADVANCED RESEARCH PROJECTS AGENCY

Rand
SANTA MONICA, CA. 90406

## PREFACE

Any detailed study of the temperature in the lower atmosphere, as well as heat balance studies at the earth's surface, must necessarily consider conditions at the surface itself: e.g., the properties of the ground regarded as a medium for the transfer of heat.

This report examines the computation of ground surface temperature in the Rand two-level general circulation model with specific reference to the inclusion of soil heat flux. Comparative results of various numerical integrations are presented to determine the most realistic technique for the computation of the ground surface temperature. It is hoped that this discussion will contribute to the improvement of the accuracy of computed ground surface temperature in the simulation of climatic changes.

Related Rand reports on the dynamics of climate are R-877-ARPA, *A Documentation of the Mintz-Arakawa Two-Level Atmospheric General Circulation Model* (December 1971); R-1318-ARPA, *The Radiation and Heat Budget of the Mintz-Arakawa Model: January* (October 1973); and R-1544-ARPA, *The Radiation and Heat Budget of the Mintz-Arakawa Model: July* (forthcoming).

## SUMMARY

The computation of ground surface temperature in the Rand two-level atmospheric general circulation model has been examined with specific reference to the inclusion of soil heat capacity as well as soil heat flux.

In the control experiment, a global ground surface temperature distribution was calculated by solving the heat balance equation at the earth-atmosphere interface, assuming a zero soil heat capacity as well as zero heat flux into the soil by conduction. The results based on 48-hour integration of the model for January show the following:

1. The daily maximum surface temperature is too high, especially in equatorial and tropical regions of both the summer and winter hemispheres.
2. The amplitude of the diurnal temperature oscillation is unrealistic in these regions.
3. There is no time lag between the maximum solar radiation and the maximum ground surface temperature.

The computation of ground surface temperature (bare land only) was repeated with the same conditions (e.g., zero heat capacity) as those in the control experiment *except* that an explicit parameterized formulation for soil heat flux was included in the heat balance equation. The results of these experiments showed relatively lower amplitudes of daily maximum surface temperature as well as diurnal range. However, the maxima in soil heat flux, solar radiation, and ground temperature occurred at the *same* local time. This feature is at variance with observations, which show that the maximum in soil heat flux precedes the maximum in solar radiation by 2 hours and the maximum in ground temperature by 3 hours.

The model was then integrated to compute ground temperature by solving a prognostic equation that included nonzero soil heat capacity as well as soil heat flux. The results of this experiment showed the

most realistic distribution of ground surface temperature with respect to amplitudes of ground temperature and diurnal range, as well as phase relationship between the ground temperature, solar radiation, and soil heat flux.

## ACKNOWLEDGMENTS

Sincere appreciation is extended to E. S. Batten and M. E. Schlesinger for very forthright and illuminating discussions. The formula for the soil heat flux used in Experiment 4 was pointed out to the author by E. S. Batten. David Pass was responsible for performing the numerical integrations of various experiments. The author is thankful to W. L. Gates and Carl Gazley, Jr., for reviewing the manuscript.

C[illegible]ENTS

## SYMBOLS

$C_D$ = surface drag coefficient

$C_H$ = sensible and latent heat flux parameter

$C_p$ = specific heat of air at constant pressure

$c$ = volumetric heat capacity of the soil

$D$ = damping depth

$G$ = soil heat flux

$GW$ = dimensionless measure of ground wetness

$H$ = sensible heat flux from the surface

$L$ = latent heat of evaporation

$LE$ = latent heat flux from the surface

$q_s$, $q_4$ = respectively, mixing ratios at the surface and in air just above the ground

$R$ = net long-wave radiation emitted from the surface

$R_N$ = net radiation

$S$ = total solar radiation absorbed by the ground

$T_4$ = air temperature at anemometer level

$T_D$ = soil temperature at depth D

$T_g$ = ground surface temperature

$T_s$ = soil temperature

$\bar{T}$ = average daily soil temperature, assumed same at all depths

$|\vec{V}_s|$ = measure of surface wind speed

$\Delta t$ = time interval of integration

$\lambda$ = thermal conductivity of the soil

$\mu$ = empirical parameter ($= G/R_N$)

$\nu$ = Stefan-Boltzmann constant

$\rho_4$ = density of air at anemometer level

$\sigma$ = dimensionless vertical coordinate, $0 \leq \sigma \leq 1$, increasing downward

$\omega$ = frequency of diurnal oscillation

# I. INTRODUCTION

## SIGNIFICANCE OF GROUND SURFACE TEMPERATURE

The heat flux and the temperature distribution at the ground surface and in the soil, down to a depth where temperature waves are damped to a negligible amount, are subjects of considerable importance to many meteorological problems. Meteorologically, the ground surface (as the lower limit of the atmosphere) is an intermediary for the energy exchange between the atmosphere and the underlying surface. One of the important heat sources affecting the atmospheric circulation is the transfer of sensible and latent heat between the surface and the atmosphere. The direction of the energy flow across the interface is primarily determined by the difference between the ground surface temperature and the air temperature immediately above it. Thus in studies of atmospheric circulation it is necessary to know the ground surface temperature accurately.

## FACTORS DETERMINING THE GROUND TEMPERATURE

The observed temperature field at the ground (and within the soil) is the result of a number of complex factors. The factors can be grouped into two general categories: the external and the intrinsic. The external factors are meteorological elements, such as radiation, rain, snow, air temperature, humidity, and heat transfer by the wind. Although the relative importance of each of these varies, the radiation balance generally is dominant. The intrinsic factors are the properties of the soil itself, such as the texture, moisture content, topography (including slope and altitude), and vegetation cover. There are also the special effects of an urban environment and of fires. It is evident that to understand the ground temperatures, both the external and intrinsic factors and their interrelationships must be taken into consideration.

## RESEARCH STATUS

### Observational

The literature contains extensive descriptions of the surface temperature characteristics based upon *observations*. These include the variations of the surface temperature, the amplitude and time of maximum ground temperature, and the effects of surface cover on the surface temperature. Geiger (1965) has discussed these factors in considerable detail in his treatise *The Climate Near the Ground*. However, it is also seen that observational records are quite scarce and the distribution of ground temperature measuring stations over the earth's surface is very uneven. There is no universally uniform practice of measurement; most frequently the methods of observation are determined by needs. As a consequence, the representativeness and accuracy of available data are uncertain, and the results based on these data are usually approximate and not necessarily mutually consistent (Sutton, 1953).

### Theoretical

In the field of energy-transfer climatology, there is a long history of modeling based upon analytical solutions to sets of differential equations (see, for example, Ingersoll et al., 1948; Brunt, 1934; Lettau, 1951; Eckert and Drake, 1959; Lonnquist, 1962).

In solving the heat balance equation at the earth-soil interface, conduction is the most important process of heat transfer in the soil. Although soil is not a homogeneous medium and there are other mechanisms of heat transfer in the soil, the Fourier theory of heat conduction does, in most cases, apply to real conditions in the atmosphere (Chang, 1958). Though the rigorous theoretical treatment of heat conduction in soil is outside the scope of this study, we have given in the Appendix a general outline of the procedure to obtain the analytic solution to the heat conduction equation (Eq. (A-3)) as well as an expression for soil heat flux (Eq. (A-6)).

The analytic solutions of the heat-budget equation of the earth's surface have been discussed by Lettau (1951), who has developed a

theoretical model of surface temperature oscillations. This model gives the amplitudes and phase lags of both the diurnal and annual courses in terms of external conditions and the physical properties of the soil and atmosphere. The solutions of this and various other analytical models indicate the following characteristics of the surface temperature.

1. For zero heat capacity there is *no* time lag between the ground temperature and the soil heat flux.
2. For non-zero heat capacity, the soil heat flux leads the surface temperature by 3 hours for diurnal course and 1.5 months for annual cycle.
3. The amplitude of surface temperature also depends upon heat capacity; for zero heat capacity, the amplitude cannot show any appreciable decrease.

In more recent meteorological research, the ground surface temperature is usually computed by solving the earth-atmosphere interface heat balance equation with the assumption of continuity of the interface temperature. These computations are generally made as a part of more complex atmospheric circulation models--both boundary layer models (Estoque, 1963; Pandolfo et al., 1965; Sasamori, 1970) and general circulation models (Manabe et al., 1965; Gadd and Keers, 1970; Gates et al., 1971; Delsol et al., 1971; Kasahara and Washington, 1971). The basic assumptions are that the heat capacity of the earth is zero and that there is no *net* heat flux through the air-earth interface. Recently it has been proposed in some general circulation models (Corby et al., 1972; Arakawa, 1972) to compute the ground temperature by solving a prediction equation. Myrup (1969) and Outcalt (1972) have developed a digital surface-climate simulator model to study diurnal surface thermal and energy transfer regimes. Their models are based on the equilibrium temperature theory, which states that given a set of astronomical-temporal atmospheric and surface boundary conditions, there is one and only one surface temperature which balances the energy conservation equation across the surface of the earth. Jacobs

and Brown (1973) use a heuristically derived iterative technique to solve the *quartic* form of the heat balance equation in order to obtain an equilibrium surface temperature.

The ground temperature values obtained in the above-mentioned works have been discussed at length in the literature; the results necessarily reflect the assumptions of the model. For example, Sasamori (1970) has reported that the predicted surface temperatures are higher than observed; he attributes this discrepancy to the assumption of no horizontal temperature advection. Estoque (1963) also reported his model's tendency to overestimate the soil heat flux during most of the day but to underestimate it about midday. The general circulation models (Gates et al., 1971) indicate highly unrealistic values of the ground surface temperature as well as the diurnal variation, especially in African and South American regions.

Computational

Apart from some variations in the formulations of the components of the heat balance equation among different models, the most noteworthy characteristics of the incorporation of heat flux in the soil are as follows:

1. While a number of local atmospheric and soil boundary layer models include soil heat flux *explicitly*, only Delsol et al. (1971) have done so in a general circulation model.

2. Some general circulation models (Gates et al., 1971; Manabe et al., 1965) have completely neglected the soil heat flux as well as soil heat capacity.

3. Other general circulation models use a parameterized technique to compute soil heat flux. For example, Kasahara and Washington (1971) specify that soil heat flux is three-tenths of the sensible heat flux into the atmosphere; Gadd and Keers (1970) consider soil heat flux to be a fraction of the *net* radiation flux. Corby et al. (1972) who use a prognostic equation include soil heat capacity in the equation but do not compute soil heat flux explicitly.

PURPOSE

The purpose of this research is to examine the computation of ground surface temperature in an atmospheric circulation model with specific reference to the inclusion of soil heat flux. We propose to use the existing version of Rand's two-level general circulation model to compute the ground temperature. Various numerical integrations will be performed by using different formulations of soil heat flux, and by solving a time dependent equation for the ground temperature which includes soil heat flux as well as soil heat capacity. The results will be compared to determine the most realistic method for the computation of the ground surface temperatures.

## II. THE BASIC CIRCULATION MODEL

The basic model equations used in this study are those described in a comprehensive description and documentation of a two-level atmospheric general circulation model by Gates et al. (1971). The original model of Mintz and Arakawa has been adapted by Rand to simulate global climate, as well as to test atmospheric predictability, and has undergone a series of modifications and improvements. Figure 1 shows a schematic cross section of the two-layer model. The model equations are set in the so-called $\sigma$ coordinate system in which the earth's surface is always the coordinate surface $\sigma = 1$. Here $\sigma$ is the dimensionless vertical coordinate given by $\sigma = (p - p_t)/(p_s - p_t)$, where p is the pressure, $p_t$ is the (constant) tropopause pressure, and $p_s$ is the (variable) surface pressure. The results of numerical experiments with the model have been described and discussed by Gates (1972). What follows is based on these two Rand reports.

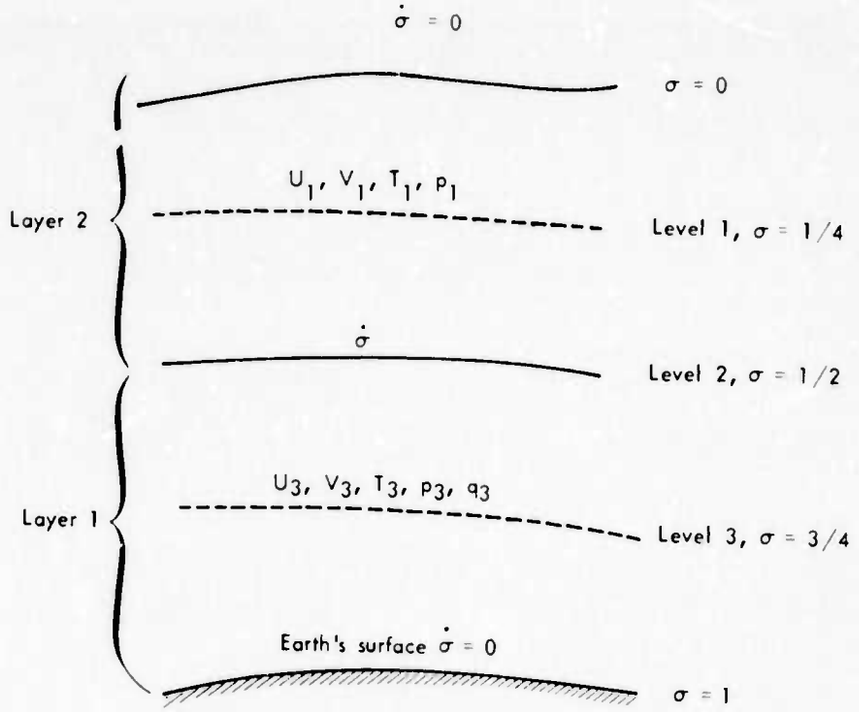


Fig. 1 — Schematical vertical representation of the model

The model computes horizontal wind velocity, temperature, and pressure at each of the two levels 1 and 3, which approximate the 400-mb and 800-mb surfaces. The mixing ratio is presently computed *only* at the lower level 3. The vertical motion is given by $\dot{\sigma}$; it is determined at a central level ($\sigma \approx 600$ mb) and is prescribed to be zero at the top of the model atmosphere ($\sigma = 0$, $p \equiv 200$ mb) and at the earth's surface ($\sigma = 1$).

The diabatic heating in the model is provided by the net radiation, the release of latent heat, and sensible heat transfer from the surface. The radiative heat transfer is itself affected by water vapor and clouds, with the latter determined as a result of both large-scale and convective processes. The moisture source is provided by the evaporation, and the sink is the precipitation released in both the large-scale and cumulus scale condensation.

A thin boundary layer (with subscript 4) is assumed at the air-ground interface. This in effect implies that the quantities with subscript 4 apply to the anemometer level in the atmosphere. The parameters at the ground surface are signified by the subscript g. It may be remarked here that the quantities at level 4 (top of atmospheric boundary layer) are *not* predicted; instead they are obtained from the predicted values of the quantities at levels 1 and 3. The ground surface temperature is determined by solving the heat balance equation at the air-ground interface. Over the oceans, the sea surface temperature is prescribed and held fixed throughout the simulation.

The grid spacing in the horizontal is 4° latitude and 5° longitude. The finite difference approximations have been described in detail by Gates et al. (1971). The time integration proceeds in steps of 6 minutes (= $\Delta t$); the forcing terms of the governing equations are computed every half hour (i.e., every fifth time step). For all other relevant details about the basic circulation model, the reader is referred to Gates et al. (1971) and Gates (1972).

## III. SOLUTION OF THE HEAT BALANCE EQUATION WITHOUT SOIL HEAT FLUX: THE CONTROL EXPERIMENT

As indicated in the Introduction, we planned a series of experiments to determine the effect of soil heat flux on the ground surface temperature. Accordingly, we first integrated the basic circulation model *without* incorporating the soil heat flux in ground surface temperature computations. This is designated as the control experiment. Thus for the control experiment we computed the ground temperature by solving the heat balance equation

$$R + H + LE - S = 0 \tag{1}$$

at the earth-atmosphere interface. Here R is the net long-wave radiation emitted from the surface; H and LE are, respectively, the sensible and latent heat fluxes from the surface; and S is the total solar radiation absorbed by the ground. As described by Gates et al. (1971), the heat flux components (except for S) depend upon ground temperature (both at time $t + \Delta t$ as well as time t). Thus, throughout this study, we use backward implicit method for computing ground surface temperature. In this study, since there is more emphasis on comparison between different experiments rather than absolute results of any one, we have used *exactly the same* formulations for H and LE as in Gates et al. (1971). Thus substituting for R, H, and LE in Eq. (1) and rearranging, we obtain the following expression for computing the ground temperature at time $t + \Delta t$:

$$T_g^{t+\Delta t} = \frac{S - R + C_H T_4 + \frac{LC_H}{C_p}\left\{q_4 + GW\left[\frac{dq_s(T_g)}{dT} T_g - q_s(T_g)\right]\right\}}{C_H\left[1 + \frac{L}{C_p} GW \frac{dq_s(T_g)}{dT}\right]} \tag{2}$$

(omitting superscript t from terms on the right-hand side). Here

$$C_H = \rho_4 C_D C_p |\vec{V}_s|$$

where $\rho_4$ = density of air at anemometer level (level 4)

$C_D$ = surface drag coefficient

$C_p$ = specific heat of air at constant pressure

$|\vec{V}_s|$ = measure of surface wind speed

$T_g$ = (appearing on right-hand side) ground surface temperature at time t

Also $T_4$ = air temperature at anemometer level

$L$ = latent heat of evaporation

$q_s, q_4$ = mixing ratios at the surface and in air just above the ground

GW = dimensionless measure of ground wetness taking values from 0 (for dry conditions) to 1 (for completely wet conditions)

The sign convention preceding the symbols in Eq. (1) is chosen so that it is positive when the flux is away from the ground and negative when it is toward the surface. Equation (1) is formulated according to the law of conservation of energy, assuming that the earth's surface contains no heat but that a considerable exchange of heat occurs across it. It may be noted that Eq. (1) also assumes horizontal homogeneity so that only vertical heat transfer is considered; horizontal advection is of considerable importance in nature when two different kinds of surfaces exist side by side and where ground is put to different uses. For the purposes of our experiment, we apply Eq. (1) over bare land, snow-covered land, or ice-covered land. For ice-covered ocean, the surface heat balance equation is modified by the addition of a term to include conduction of heat through the ice; over the ocean itself we prescribe the sea surface temperature.

With initial and boundary conditions appropriate to January, the two-level model was integrated for a period of 48 hours. The ground temperature was calculated by using Eq. (2). The results of the control experiment have been compared with other experiments by comparing

daily maximum surface temperatures and the diurnal range of surface temperature at all non-oceanic points of the grid. For more detailed analysis, we selected three representative land points over the globe, as shown in Fig. 2, which also shows the land areas of the globe as resolved by the model.

Figure 3 shows the global distribution of daily maximum ground surface temperature as simulated by the model for the month of January. The realism of this distribution cannot be ascertained for want of global daily ground surface temperature maps. However, an effort will be made to draw inferences on the basis of available information.

## MAGNITUDE OF MAXIMUM SURFACE TEMPERATURE

There are very few records of maximum surface temperature for natural surfaces, although estimates have been made of the maxima of surface temperature as a function of the air temperature at the conventional thermometer shelter level. For example, Johnson and Davies (1927) estimated that in the hottest areas of the globe the surface temperature cannot exceed 90°C. This was based on an air temperature of 60°C at a height of 20 cm above the ground. However, there is no direct evidence of any natural surface temperature as high as this. Also, considering that convective processes, which have a regulating influence on the temperature, become more efficient for high surface temperatures, it is doubtful whether substantially higher surface temperatures can in fact be reached. These estimates also do not take into account other factors that influence the surface temperature, such as the effect of water content on the thermal conductivity of the soil and the movement of air over the surface.

In view of the above, it is reasonable to expect that maximum "natural" surface temperatures generally do not exceed 60°C in the winter hemisphere. Consequently we infer that the control experiments results show an unrealistic distribution of ground surface temperatures in the continental areas south of 30°N, i.e., in the tropical region of winter hemisphere and in the entire summer hemisphere. Specifically, in the Sahara region, the distribution is more typical of late spring/early summer rather than January (in May, the highest temperature of

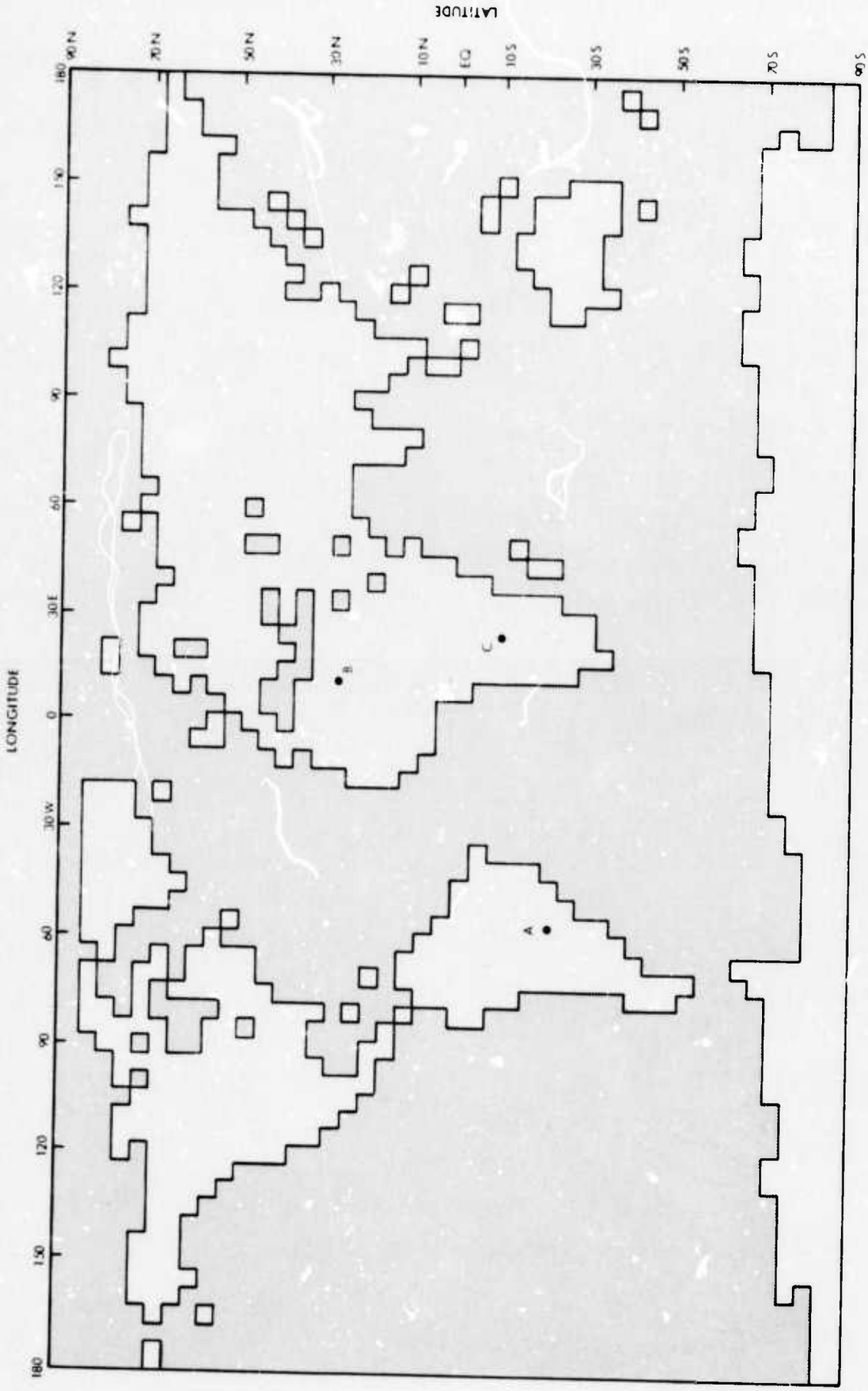


Fig. 2 — Land areas as resolved by the model grid, and the locations of selected points A, B, and C

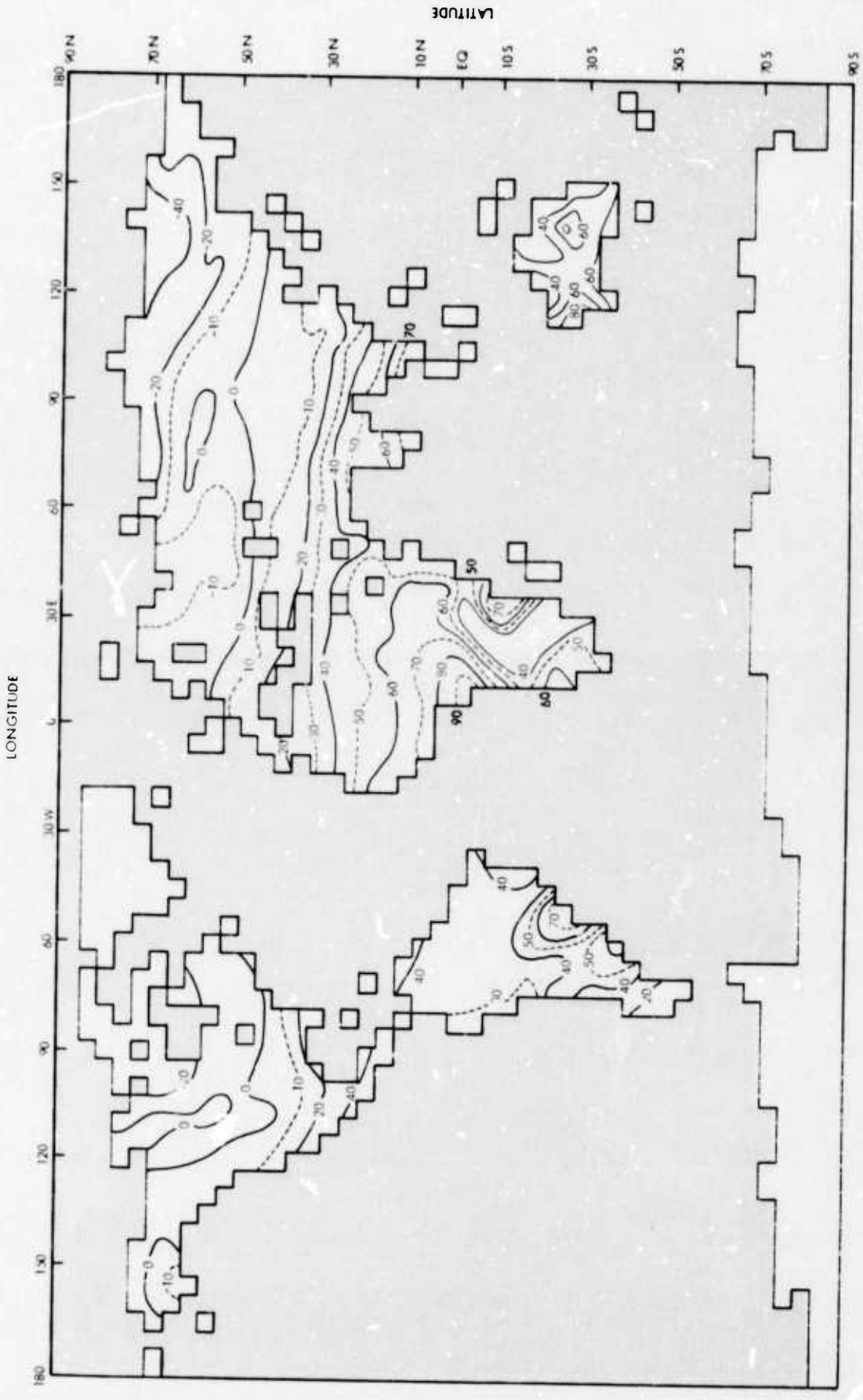


Fig. 3 — Daily maximum ground surface temperature (°C) - Control experiment (January)

73°C was recorded in Sahara) (Geiger, 1965). Similarly, temperatures of 90°C in equatorial Africa appear to be too high; since this is a very wet and forested region, it is highly unlikely that such a high value for maximum surface temperature could be attained in nature.

Physically, the maximum and minimum surface temperature is reached when the flow of heat into the soil exactly balances the flow outward; the actual value attained depends not only on the radiation, evaporation, and heat transfer in the air but also on the heat transfer in the soil. Since we have not incorporated the heat transfer in the soil in Eq. (1), it seems likely that this exclusion is largely responsible for the "unrealistic" distribution of ground surface temperature found in the control experiment.

## DIURNAL RANGE OF GROUND SURFACE TEMPERATURE

Figure 4 shows the global distribution of the diurnal range of the surface temperature obtained in the control experiment. In nature the amplitude of the surface diurnal variation changes considerably, particularly with the time of the year. In winter, the daily temperature oscillation at the surface is much smaller than in summer (Fig. 5). Other observations (Geiger, 1965) show that at Pavlosk (60°N) the diurnal range in summer is 15°C while in winter it is about 2 or 3°C. In Central Europe (Vienna) the amplitudes for winter and summer are 3°C and 22°C, respectively. In general, outside the tropics, for clear days and bare surface, 25°C is a fairly representative value of diurnal oscillation in summer (Sutton, 1953). In winter this value is about 2 or 3°C. It can be seen from Fig. 4 that the diurnal oscillation values for the control experiment are rather unrealistic, exceeding 50°C in South America. Also, within summer tropical regions, observations (Sinclair, 1922) have shown a diurnal range of 56°C in the extreme, whereas the control experiment shows a diurnal range in excess of 70°C over wide areas of tropical regions, even in the winter hemisphere. Thus, although in general the diurnal oscillations obtained in the control experiment are not realistic, the model at least attempts to include the nature of the surface and the state of the sky, both of which affect the amplitude of diurnal variation of the surface temperature.

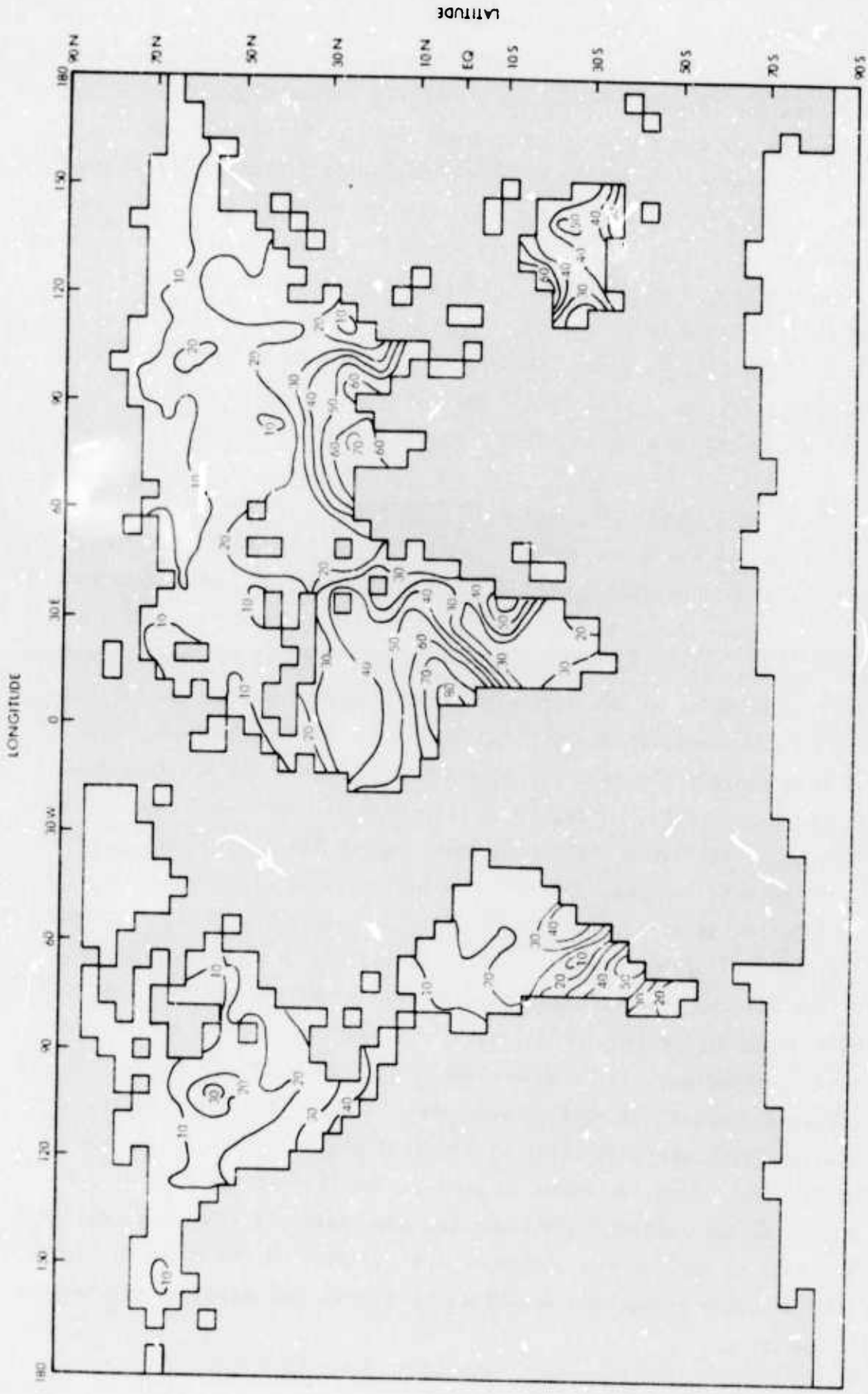


Fig. 4 — Diurnal range of ground surface temperature (°C) - Control experiment (January)

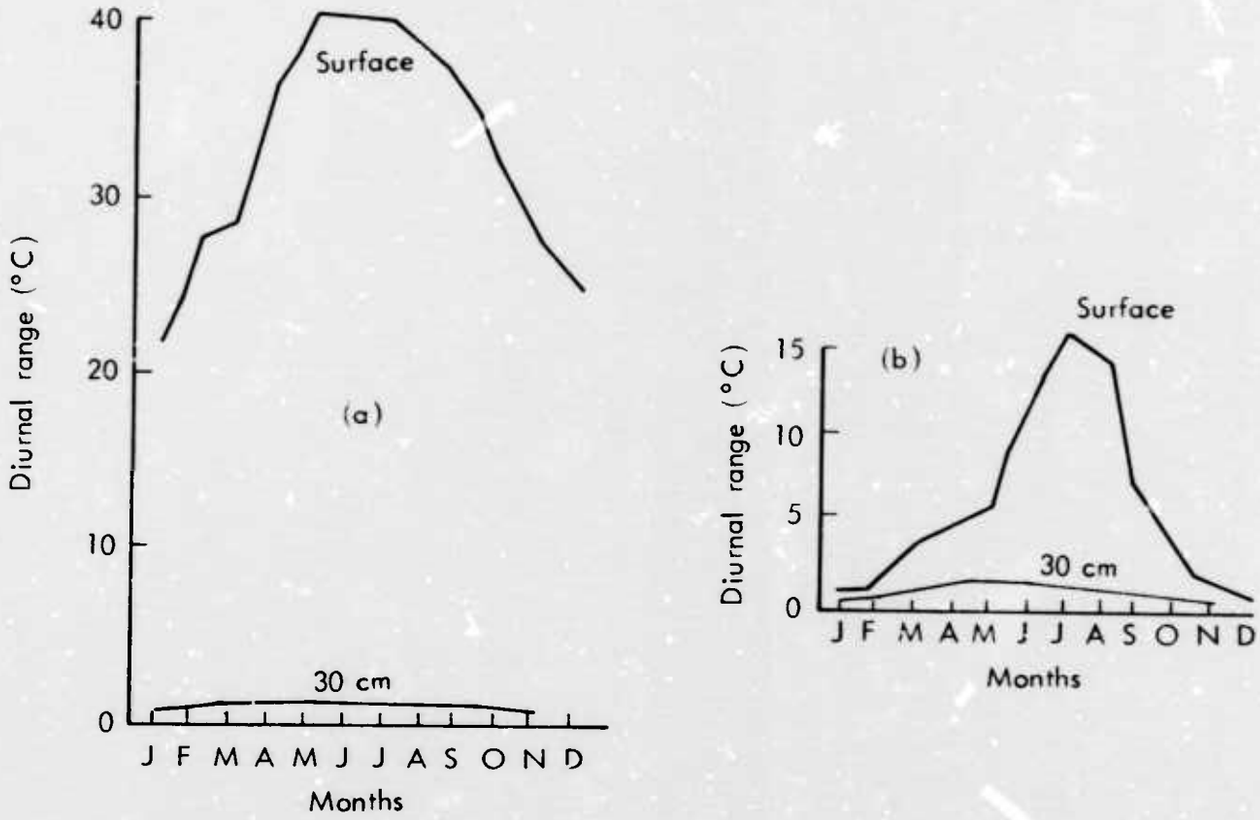


Fig. 5 — Annual course of diurnal range in soil temperature at (a) Giza, Egypt (b) Zurich, Switzerland (from Chang, 1958)

The *time of maximum surface temperature* is also of considerable interest in analysis of heat transfer in the atmosphere. Observations have shown that on clear days the surface attains its maximum temperature about 1 hour after the time of maximum solar radiation (Lonnquist, 1962; Sutton, 1953, p. 197). It may be mentioned here that this lag of the daily maximum temperature increases with depth in the soil. Figure 6 shows a plot of computed ground temperature and solar radiation as a function of local time at two selected locations (A and B) of the grid. It is seen that there is *no* time lag between maximum solar radiation and maximum ground temperature. This result also follows from the analytical solutions and is to be expected when heat capacity is neglected.

In summary, the results of the control experiment show that

1. The daily maximum surface temperature is too high, especially in equatorial and tropical regions of both the summer and winter hemispheres.
2. The amplitude of the diurnal temperature oscillation is unrealistic in these same regions.
3. There is no time lag between the maximum solar radiation and the maximum ground surface temperature.

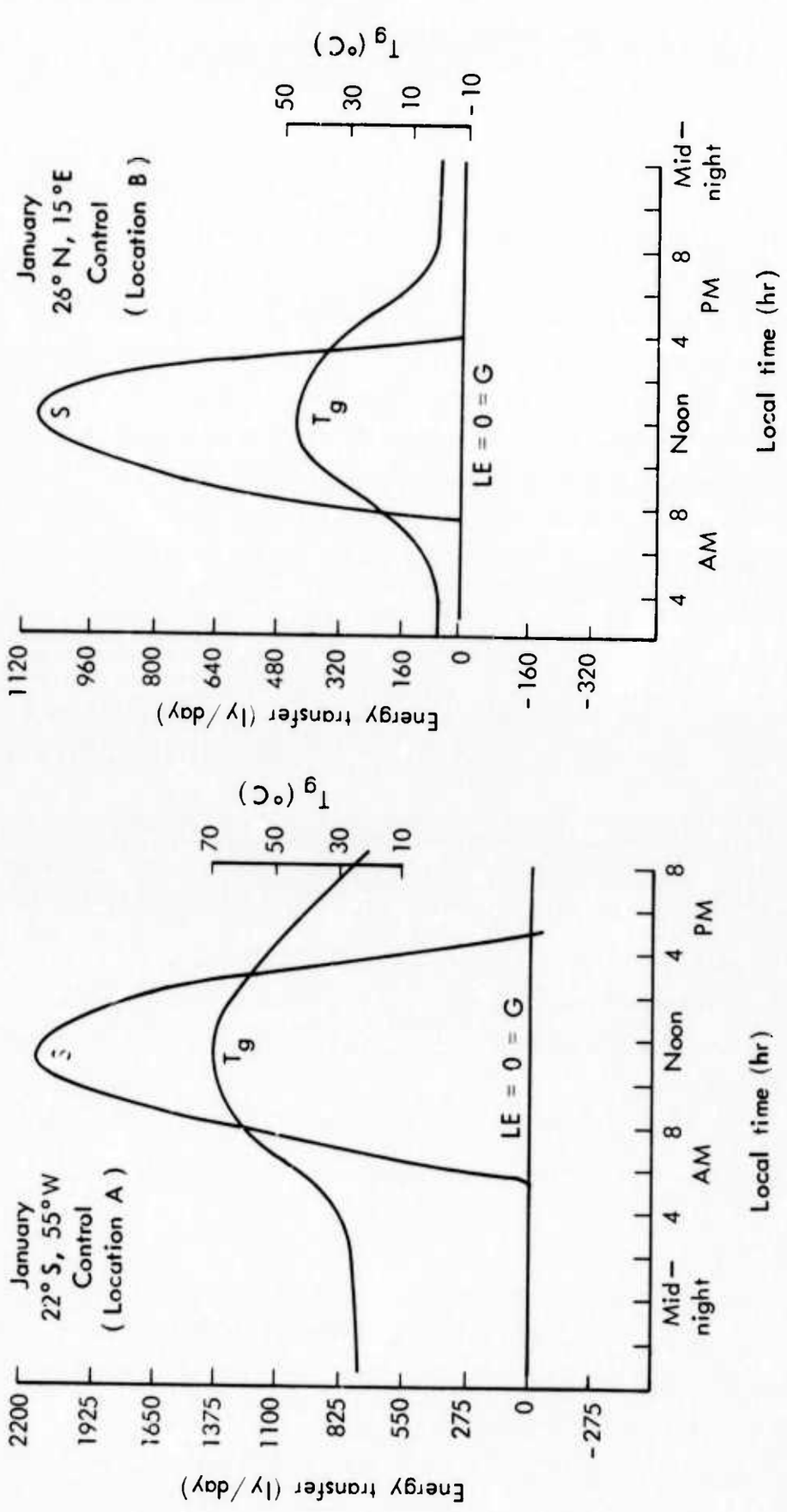


Fig. 6 — Daily ground temperature ($T_g$ °C) and solar radiation (S, ly/day) as a function of local time at two selected locations for the month of January

## IV. SOLUTION OF HEAT BALANCE EQUATION INCLUDING SOIL HEAT FLUX: EXPERIMENTS 1 TO 3

In the previous section we have described the ground surface temperature as calculated in the control experiment with the Rand two-level atmospheric circulation model. In this section we describe the results of a series of numerical experiments which were performed to determine the effect, on the ground surface temperature, of incorporating the soil heat flux at the surface, assuming zero heat capacity of the ground itself. (The situation when the heat capacity is not zero is considered subsequently in Sec. V.)

In these experiments the ground surface temperature was obtained as a solution of the generalized heat balance equation

$$R + H + LE + G - S = 0 \qquad (3)$$

where R, H, LE, and S have the same meaning and formulations as in the control experiment (Eq. (1)), and G is the soil heat flux at the surface. Equation (3) was solved for bare land points only. Table 1 shows the formulation of G used in the various experiments.

### Experiment 1

The rate at which heat flows through soil at a depth z is determined by the thermal conductivity and the temperature gradient at that level. Thus at z = 0 (surface), the soil heat flux G may be computed from the expression

$$G = \lambda \left( \frac{\partial T}{\partial z} \right)_{z=0}$$

where $\lambda$ is the (constant) thermal conductivity. Strictly speaking, this equation cannot be applied to real soils because they are not homogeneous. But for most purposes it holds when an appropriate value of $\lambda$ is chosen (de Vries, 1963).

Table 1

FORMULATIONS OF SOIL HEAT FLUX G USED FOR COMPUTING GROUND SURFACE TEMPERATURE WITH EQ. (3)

| Experiment | Formula for Soil Heat Flux G | Reference |
|---|---|---|
| Control | G = 0: no flux | --- |
| 1 | $G = \frac{\lambda}{D}(T_g - T_D)$ | Estoque (1963), (L); Pandolfo (1965), (L); Myrup (1969), (L); Delsol et al. (1971), (GCM); Sasamori (1970), (L) |
| 2 | $G = \mu R_N$ | Gadd and Keers (1970), (GCM) |
| 3 | G = 0.3H<br>LE = H | Kasahara and Washington (1971), (GCM) |

NOTE: In reference column, L = local atmospheric and soil boundary layer models; GCM = atmospheric general circulation models.

SYMBOLS: $\lambda$ = thermal conductivity

$T_g$ = ground surface temperature

D = damping depth

$T_D$ = soil temperature at depth D

$R_N$ = net radiation

$\mu = G/R_N$: empirical parameter

Since our circulation model does not have explicit levels within the soil, we approximate the above expression for G as

$$G = \lambda \frac{T_g - T_D}{D} \tag{4}$$

where $T_g$ is the temperature of ground surface, and $T_D$ is the temperature of soil at depth D (at which the diurnal variations become negligible). The values of $T_g$ which can be obtained by using Eq. (4) in

Eq. (3) are dependent upon the values assigned to $\lambda$, $T_D$, and D. Table 2 shows the values of these quantities used in some numerical models. It may be noted that Eq. (4) is an approximate form of Eq. (A-6) of the Appendix if we neglect the heat capacity.

Table 2

VALUES OF D, $T_D$, $\lambda$ USED IN SOME NUMERICAL MODELS

| Model Type | D (cm) | $T_D$ (°K) | $\lambda$ (cal $cm^{-1}$ $sec^{-1}$ $deg^{-1}$) | Reference |
|---|---|---|---|---|
| Local boundary layer | 50 | 294.14 | $1.44 \times 10^{-3}$ | Estoque (1963) |
| | 50 | 295 | $0.8 \times 10^{-3}$ to $1.9 \times 10^{-3}$ | Pandolfo (1965) |
| | 20 | 294.3 | $2.6 \times 10^{-3}$ (rural areas)<br>$9.3 \times 10^{-3}$ (urban areas) | Myrup (1969) |
| General circulation | 500 | 280 | $2.1 \times 10^{-3}$ | Delsol et al. (1971) |

The thermal conductivity $\lambda$, which is very important in estimating the soil temperature, depends upon the porosity, moisture, and organic matter content of the soil (Chang, 1958). De Vries (1963) has shown that $\lambda$ can be estimated from theoretical considerations as a function of the moisture content of the soil. The results of his calculations agree well with observed soil temperatures. In Experiment 1, we specify $\lambda$ (Fig. 7) as a function of surface moisture, represented by the ground wetness parameter GW in our model: $\lambda$ varies from $1.2 \times 10^{-3}$ for dry soil (GW = 0) to $6.0 \times 10^{-3}$ for GW $\geq$ 0.2. These values correspond closely to those given by Priestley (1959). The depth D at which the diurnal wave of soil temperature becomes negligible varies with the thermal properties of the soil. In a dry soil the temperature wave does not penetrate too far, whereas in a moderately wet soil it goes much deeper. In a thoroughly wet soil, D is the one nearest the surface (Chang, 1958). Here we specify D to vary with ground wetness GW so that D increases linearly from 10 to 50 cm as the ground wetness GW varies from 0 to 0.5. Then D decreases linearly from 50

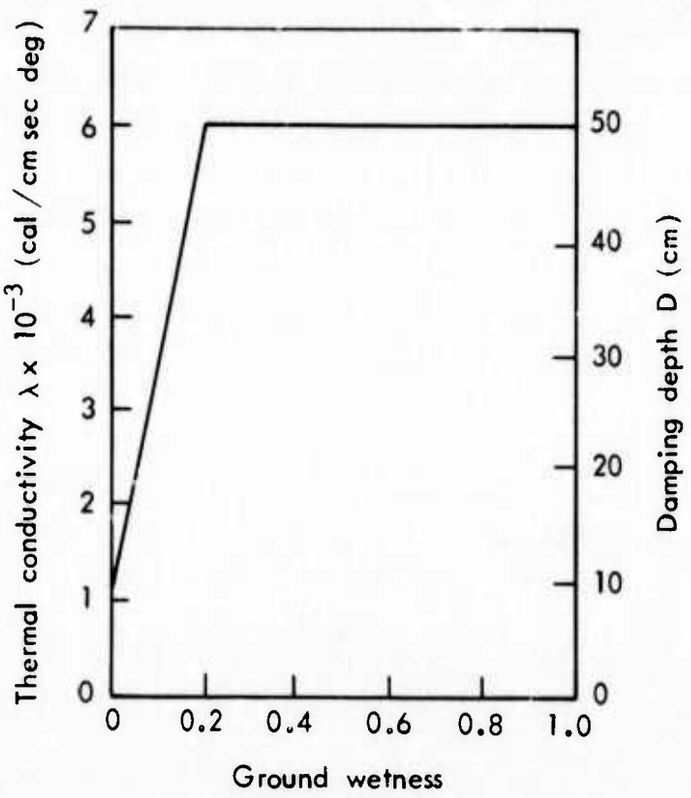


Fig. 7 — Thermal conductivity as a function of ground wetness used in Experiment 1

to 10 cm for GW = 0.5 to 1. The maximum value of 50 cm is chosen on the basis of observations, which show that for common soils the diurnal temperature wave does not penetrate below 50 cm (de Vries, 1963). We have specified $T_D$ to be 280°K at all bare land grid points.

Substituting Eq. (4) in Eq. (3) and following the same procedure as in the control experiment, we obtain an expression for computing ground temperature $T_g$ which is similar to Eq. (2) of the control experiment, except for the additional terms $(\lambda/D)T_D$ in the numerator and $\lambda/D$ in the denominator, which arise due to inclusion of the soil heat flux in the heat balance equation (3). Therefore

$$T_g^{t+1} = \frac{S - R + C_H T_4 + \frac{LC_H}{C_p}\left\{q_4 + GW\left[\frac{dq_s(T_g)}{dT} T_g - q_s(T_g)\right]\right\} + \frac{\lambda}{D} T_D}{C_H\left[1 + \frac{L}{c_p} GW \frac{dq_s(T_g)}{dT}\right] + \frac{\lambda}{D}} \qquad (5)$$

Figure 8 shows maximum surface temperature distribution for the African continent. Comparison of this with corresponding regions in Fig. 2 (control experiment) shows a general decrease in the magnitude of ground temperature. The highest value of surface temperature is 70°C, as compared to 90°C in the control run. The maximum amplitude of the diurnal range (Fig. 9) also shows a decrease of 20°C to the west and 10°C to the east. Other regions such as South America and Australia also show an improvement over control experiment results.

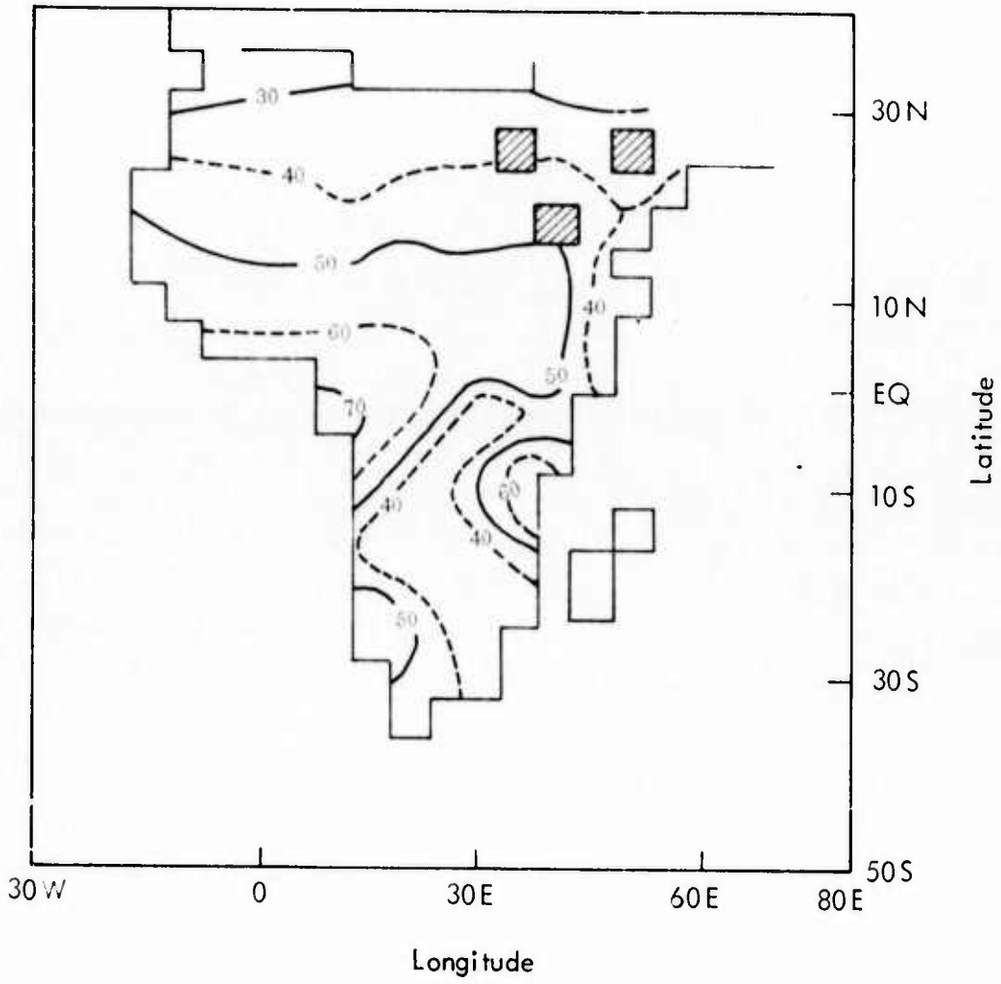


Fig. 8 — Daily maximum ground temperature (°C) for month of January (Africa) (Experiment 1)

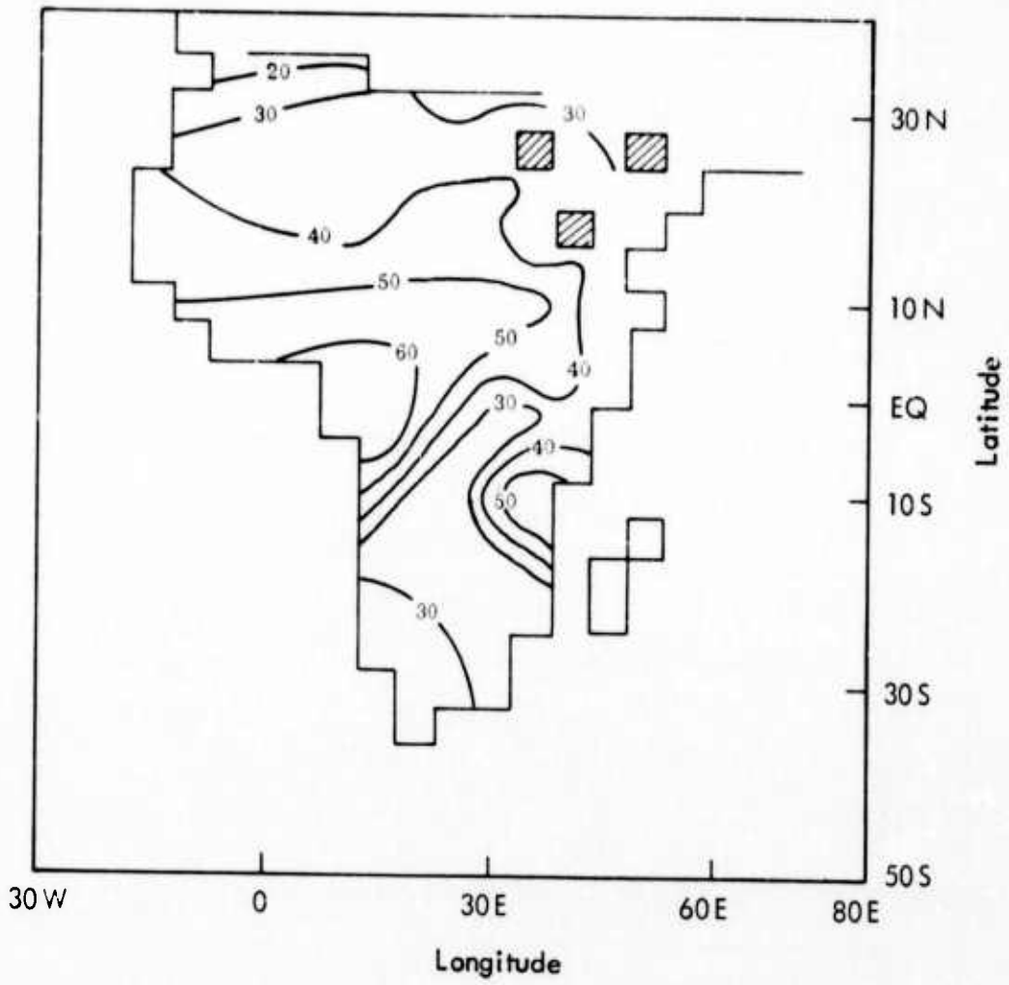


Fig. 9 — Diurnal range of ground surface temperature (°C) for month of January (Africa) (Experiment 1)

Since soil heat flux has been incorporated for only bare land points, there is no change in the patterns in the regions covered with snow/ice. Figure 10 shows the ground surface temperature variation with local time at three selected locations (A, B, and C in Fig. 2) for both Experiment 1 and the control experiment. It can be seen that the inclusion of soil heat flux G in the heat balance equation has decreased the amplitude of ground surface temperature at locations A and B appreciably. However, at location C this apparently had no effect on the ground temperature. The reason for these differences can

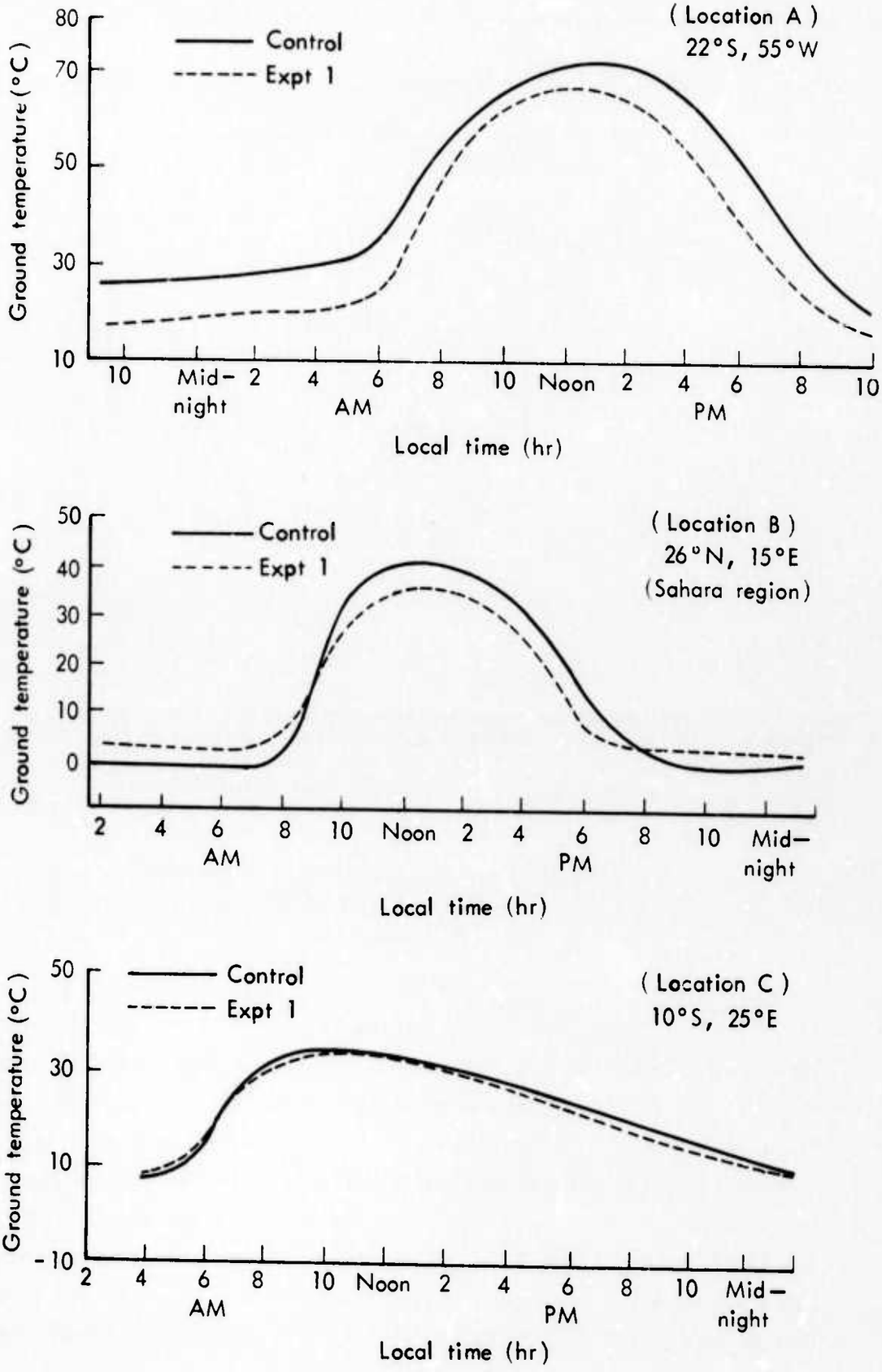


Fig.10 — Comparison of daily ground surface temperature (°C) between control and Experiment 1

be attributed to very dry surface conditions (GW ~ 0) at locations A and B but completely wet conditions (GW ~ 0.9) at location C. Table 3 shows the values of heat balance components LE, H, and G relative to the net radiation $R_N$ at locations A, B, and C for both the control experiment and Experiment 1.

Table 3

RATIO OF LE, H, AND G TO NET RADIATION $R_N$ AT LOCATIONS A, B, AND C

| | Locations A & B | | | Location C | | |
|---|---|---|---|---|---|---|
| Experiment | LE/RN | H/RN | G/RN | LE/RN | H/RN | G/RN |
| Control | ~0 | 1 | 0 | 1 | ~0 | 0 |
| 1 | ~0 | 0.6 | 0.4 | 0.9 | ~0 | 0.1 |

For the control experiment (G = 0), the ground temperature at locations A and B (LE ~ 0) was obtained as a result of balance between net radiation $R_N$ and sensible heat flux H, whereas at location C (H ~ 0) it was due to balance between $R_N$ and latent heat flux LE. For Experiment 1 (G ≠ 0), at locations A and B (LE ~ 0) G is about 40 percent of net radiation, and this contributes to lower temperatures obtained at these locations. However, at location C the balance is still predominantly between evaporation and net radiation; G is only 10 percent of $R_N$. Consequently there is no significant difference between ground temperatures obtained at C for the control experiment and Experiment 1. This shows that while heat flux into the ground is important for dry conditions (~ 40 percent of $R_N$ for bare ground), it is not very significant (~ 10 percent of $R_N$) in affecting ground temperatures for very wet conditions. These results compare well with observations (Sellers, 1965). Just as in the case of the control run, Experiment 1 also does not show a time lag between maximum solar radiation and maximum ground temperature (Fig. 11). Similarly, it may be noted that there is no time lag between maximum soil heat flux and maximum ground temperature. These results also follow from analytic

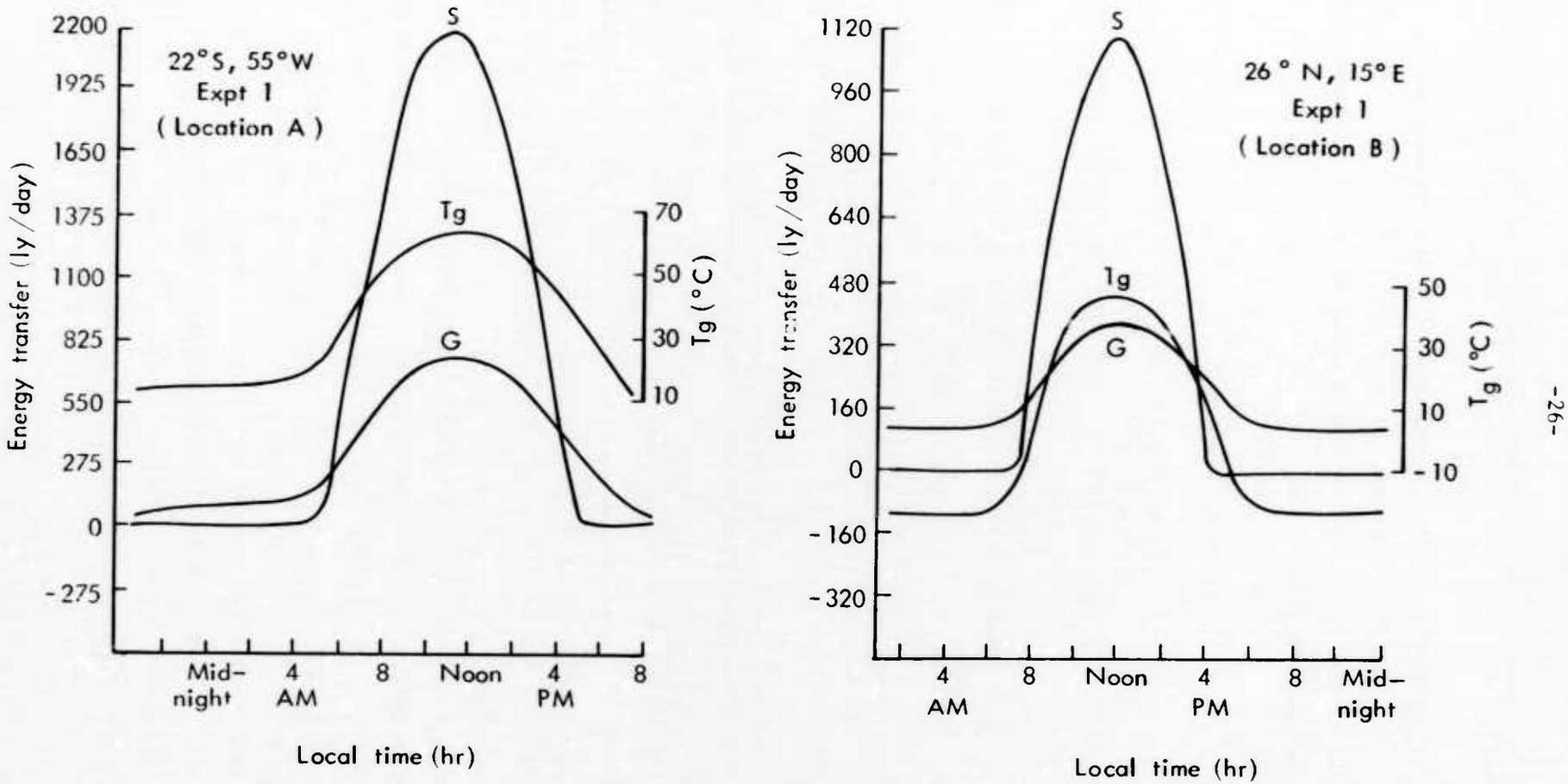


Fig.11 Daily ground temperature ($T_g$ °C) and solar radiation (S, ly/day) as a function of local time at two selected locations for the month of January (Expt 1)

treatment of the classic heat conduction equation if we neglect heat capacity. The result of Experiment 1 is at variance with conditions in nature, which show that the maximum surface temperature occurs 3 hours *after* a maximum in soil heat flux (Johnson, 1954).

Thus Experiment 1 shows that while the inclusion of soil heat flux in the heat balance equation gives relatively lower values of ground surface temperature, the relationship of ground temperature with solar radiation and soil heat flux is not realistic. The most important drawback of the formulation of G used in this experiment is the specification of *one* value for $T_D$ at all the bare land points on the globe. Moreover, the damping depth D, which can vary considerably over the globe, also has to be specified.

Experiment 2

Gadd and Keers (1970) have expressed the heat flux (G) into the ground as a fraction of net radiation ($R_N$) at the surface so that

$$\frac{G}{R_N} = \mu \tag{6}$$

where $R_N = (S - R)$; and $\mu$ is assigned a value of 0.1 for $R_N \geq 0$ (daytime) and 0.5 for $R_N < 0$ (nighttime). Thus, for Experiment 2 we obtain the ground temperature as a solution of the equation

$$H + LE - (1 - \mu)R_N = 0 \tag{7}$$

(This is obtained by substituting $G = \mu R_N$ in Eq. (3).)

An expression for computing the ground temperature $T_g$ (corresponding to Eq. (5) of Experiment 1) is thus given by

$$T_g^{t+1} = \frac{(1 - \mu)R_N + C_H T_4 + \frac{LC_H}{C_p}\left\{q_4 + GW\left[\frac{dq_s(T_g)}{dT} T_g - q_s(T_g)\right]\right\}}{C_H\left[1 + \frac{L}{C_p} GW \frac{dq_d(T_g)}{dT}\right]} \tag{8}$$

The results (Fig. 12) indicate a rather insignificant decrease in the daytime magnitude of surface temperature as compared to that of the control experiment. However, during nighttime the surface temperatures of Experiment 2 were considerably higher than those of the control experiment. These features can be attributed to two different values of $\alpha$ used in Eq. (2); lower for daytime and higher for nighttime. The values of diurnal range were also affected only to the extent that the minimum in Experiment 2 was higher than that in the control experiment. It may be mentioned here that Gadd and Keers (1970) did not compute LE and H explicitly, as we did in Experiment 2. They obtained the latent and sensible heat fluxes by partitioning the available flux ($R_N$ - G) at the surface.

Thus Experiment 2 does not improve the ground surface temperature distribution obtained in the control experiment. This may be attributed to the technique of expressing G in terms of $R_N$, which gives only a crude and indirect estimate.

Experiment 3

In their general circulation model, Kasahara and Washington (1971) computed the ground surface temperature over land or ice/snow areas by solving Eq. (3). On the basis of a study by Sasamori (1970), they prescribed the soil heat flux G to be a fraction of sensible flux H. In addition, they specified a value of *unity* to the Bowen ratio (H/LE). Thus, if we substitute

$$\left.\begin{aligned} G &= 0.3H \\ \text{and} \qquad LE &= H \end{aligned}\right\} \tag{9}$$

Eq. (3) becomes

$$R - S + 2.3H = 0 \tag{10}$$

or substituting for H in terms of ground temperature $T_g$, we obtain

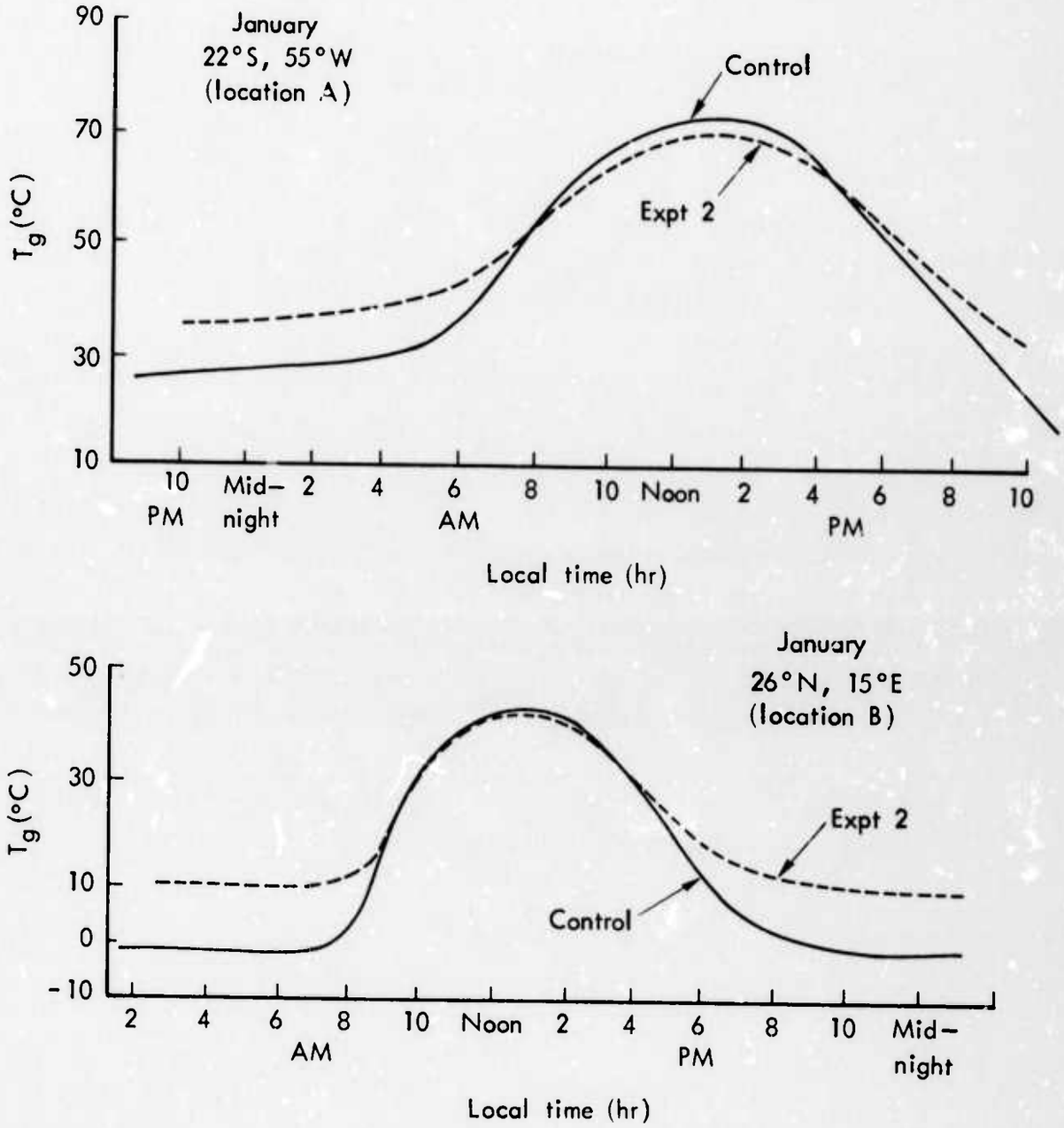


Fig.12 — Comparison of daily ground surface temperature (°C) between control and Experiment 2

$$T_g^{t+1} = T_4 + \frac{S - R}{2.3C_H} \qquad (11)$$

The results show that the values of the ground surface temperature in Experiment 3 are much smaller than those obtained in the control experiment. At some grid points, the decrease of surface temperature is as much as 20°C. Figure 13 shows a comparison of ground temperature (at two locations) between Experiment 3 and the control experiment. It can be seen that while the maximum has decreased considerably (20°C), the minimum has increased appreciably. This is reflected in smaller values (not shown) for diurnal oscillations obtained in Experiment 3.

Thus Experiment 3 gives a much improved distribution of ground surface temperature vis-à-vis the control experiment. However, the approximations for G and LE (Eq. (9)) are not quite realistic. For example, the first condition (G = 0.3H) implies that the two processes (G and H) are exactly in phase and have the same constant ratio. This is at variance with observations. Moreover, the value of 0.3 for this ratio is not universal; in fact Sasamori estimated this value for dry soil only. Again the assumption of a Bowen ratio of unity is also not realistic, because observations (Brooks and Goddard, 1966) have shown that it has a significant diurnal variation and sometimes changes sign also. It may be mentioned that Kasahara and Washington (1971) suggest a calibration of nighttime surface temperatures by controlling the ground temperature.

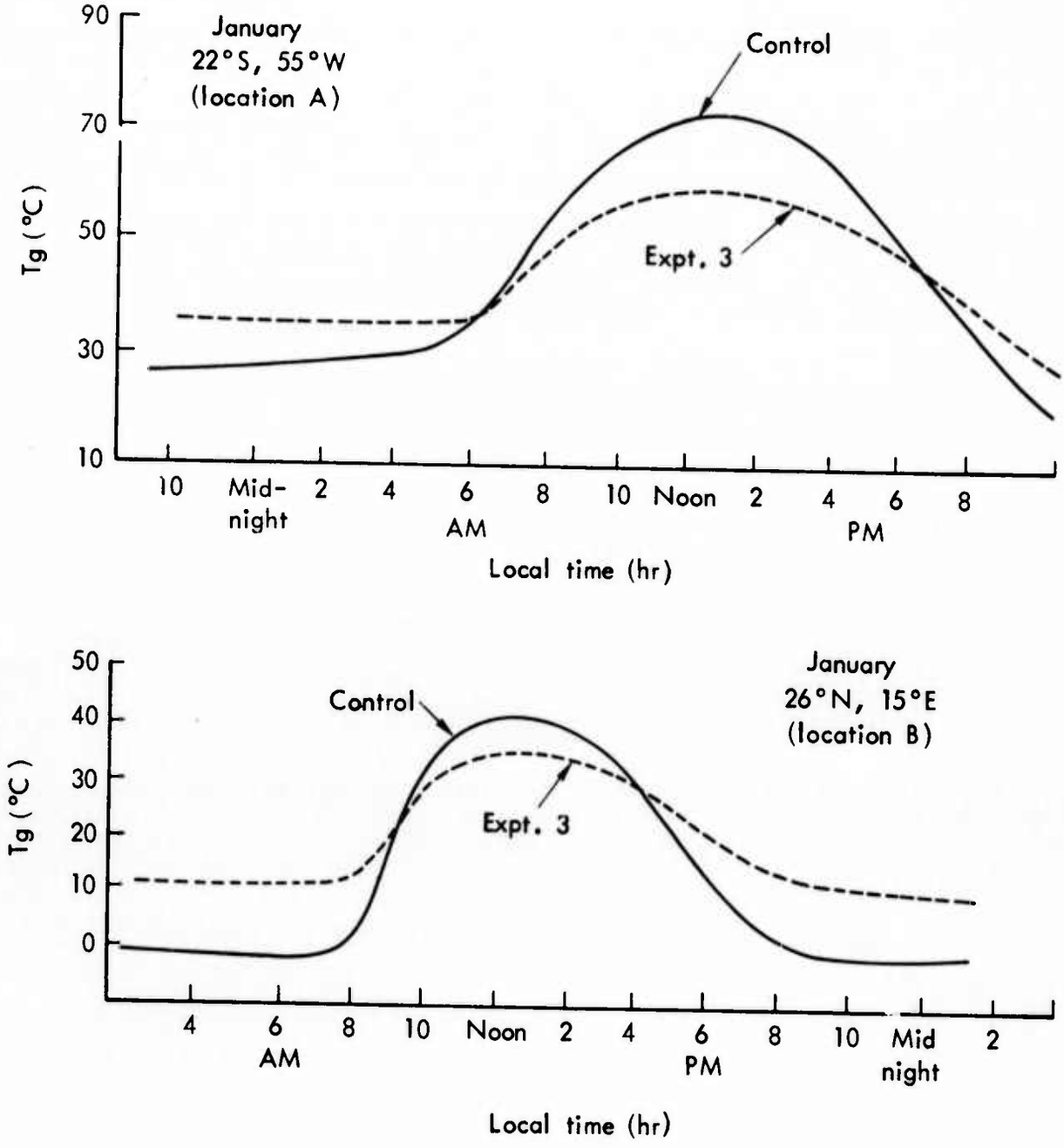


Fig. 13 — Comparison of daily ground surface temperature (°C) between control and Experiment 3

## V. PROGNOSTIC EQUATIONS FOR GROUND TEMPERATURE CALCULATIONS: EXPERIMENTS 4 AND 5

In Sec. IV we have described *three* methods of computing the ground surface temperature. These essentially involve solving the heat balance equation at the earth-atmosphere interface under the assumption of zero heat capacity. In this section we consider the situation when the heat capacity is not zero. Table 4 shows the equations used for solving for $T_g$ in Experiments 4 and 5.

Table 4

EQUATIONS USED IN EXPERIMENTS 4 AND 5

| Experiment | Basic Equation to Solve for Ground Temperature | Expression for G |
|---|---|---|
| 4 | S-R-H-LE-G = 0 | $G(0) = \sqrt{\frac{\omega c \lambda}{2}} \left[ \left( T_g^{t+1} - \overline{T} \right) + \frac{1}{\omega \Delta t} \left( T_g^{t+1} - T_g^{t} \right) \right]$ |
| 5 | $S\text{-}R\text{-}H\text{-}LE\text{-}G = c \frac{\partial T_g}{\partial t}$ | $G(1) \doteq \sqrt{\frac{\omega c \lambda}{2}} \left[ \frac{1}{\omega} \frac{\partial T_g}{\partial t} + T_g - \overline{T} \right]$ |

Hence the basic difference between Experiments 4 and 5 is that the former uses the heat balance equation to compute $T_g$, whereas the latter uses an explicit predictive equation for ground temperature $T_g$. Also, in Experiment 4, the soil heat flux G is evaluated at the surface, whereas in Experiment 5 it is approximated at a 1-cm depth in the soil. Thus while the equation used in Experiment 4 involves a non-zero heat capacity only *implicitly* through the formulation for G; the equation of Experiment 5 *explicitly* involves both soil heat capacity and soil heat flux G.

### Experiment 4

In this experiment we use Eq. (A-7) of the Appendix to represent soil heat flux (G) at the surface. Thus

$$G = \sqrt{\frac{\omega c \lambda}{2}} \left[ \frac{1}{\omega} \frac{\partial T_g}{\partial t} + T_g - \bar{T} \right] \tag{12}$$

Using an implicit technique and writing this in the notation used in Eq. (2) of the basic circulation model, we have

$$G = \sqrt{\frac{\omega c \lambda}{2}} \left[ \left( T_g^{t+1} - \bar{T} \right) + \frac{1}{\omega \Delta t} \left( T_g^{t+1} - T_g^{t} \right) \right] \tag{13}$$

Here $\omega$ is the frequency of oscillation, c is the volumetric heat capacity, $\lambda$ is the thermal conductivity, $\bar{T}$ is the average *daily* soil temperature (assumed to be the same at all depths), and $\Delta t$ is the time step of integration. Substituting this expression for G in the heat balance equation (3) and rearranging, we obtain

$$T_g^{t+1} = \frac{S - R + C_H \left\{ T_4 + \frac{L}{c_p} \left[ q_4 + GW \left( \frac{dq_s(T_g)}{dT} \right) T_g - q_s(T_g) \right] \right\} + \sqrt{\frac{\omega c \lambda}{2}} \left( \frac{T_g}{\omega \Delta t} + \bar{T} \right)}{C_H \left[ 1 + \frac{L}{c_p} GW \frac{dq_s(T_g)}{dT} \right] + \sqrt{\frac{\omega c \lambda}{2}} \left( 1 + \frac{1}{\omega \Delta t} \right)} \tag{14}$$

It can be seen that Eq. (14) is similar to Eq. (2) of the control experiment except for the last terms in both the numerator and denominator. These arise, in a way similar to Experiment 1, because soil heat flux is included in the heat balance equation. However, for the control experiment and Experiment 1 we had assumed the heat capacity c to be zero; it is non-zero for Experiment 4. For $\lambda$ we assign the same values which were used in Experiment 1 (Fig. 7). As regards c, it can be expressed as the sum of heat capacities of different soil constituents in a unit volume (de Vries, 1963); c also depends upon the moisture content. In our experiment we use a constant value of 0.6 cal $cm^{-3}$ $deg^{-1}$, which is based on the values given by Priestley (1959) and Geiger (1965). The frequency of oscillation $\omega$ is $7.27 \times 10^{-5}$ $sec^{-1}$, and $\Delta t$ is 30 min. Since the solution for $T_g$ primarily varies around $\bar{T}$, the accuracy of

the former depends to a great extent on how we treat the latter. The daily average $\overline{T}$ can be included in Eq. (14) in two ways:

1. Compute $\overline{T}$ on the basis of the "past" day's values of $T_g$ and use this average in computing $T_g$ for the following day. This technique enables us to let $\overline{T}$ vary at least on a daily basis; also it can be computed at each grid point.
2. Prescribe $\overline{T}$ as a function of latitude zones on the basis of observations. However, since there are no maps of soil temperature available on a daily basis, only monthly maps can be used. Consequently, solutions for $T_g$ for any month on a daily basis are biased toward the value of $\overline{T}$ prescribed for that month.

We integrated the model for 48 hours, using both the techniques noted above. We did not find any significant differences in the results, at least for the two days we considered. The results discussed here are based on $\overline{T}$ which was prescribed as a function of latitude zones on the basis of a map for January prepared by Chang (1958) (Fig. 14).

Figure 15 shows the distribution of maximum surface temperature for Experiment 4. Comparing this with the results of the control experiment (Fig. 2) reveals that there is considerable reduction in the magnitude of surface temperature; the most noteworthy occurring in the western half of Africa. The highest value in this case is only 60°C, whereas it was 90°C in the control run. Even in the Sahara region the range of maximum temperature is from 30° to 50°C; for the control run these values are from 30° to 70°C with 50° and 60° isotherms dominating the region. In Australia, South Asia, and South American continents also, the values tend to become more realistic. It may be noted that in this case, as also in Experiment 1, there are still rather unrealistically high values of surface temperature in the equatorial forest region of Africa. The reason for this is that during the duration of the integration of the model (48 hours) there has been no precipitation in this region and, quite contrary to a "real" atmospheric situation, there is no moisture to cause evaporational cooling. Simulation of

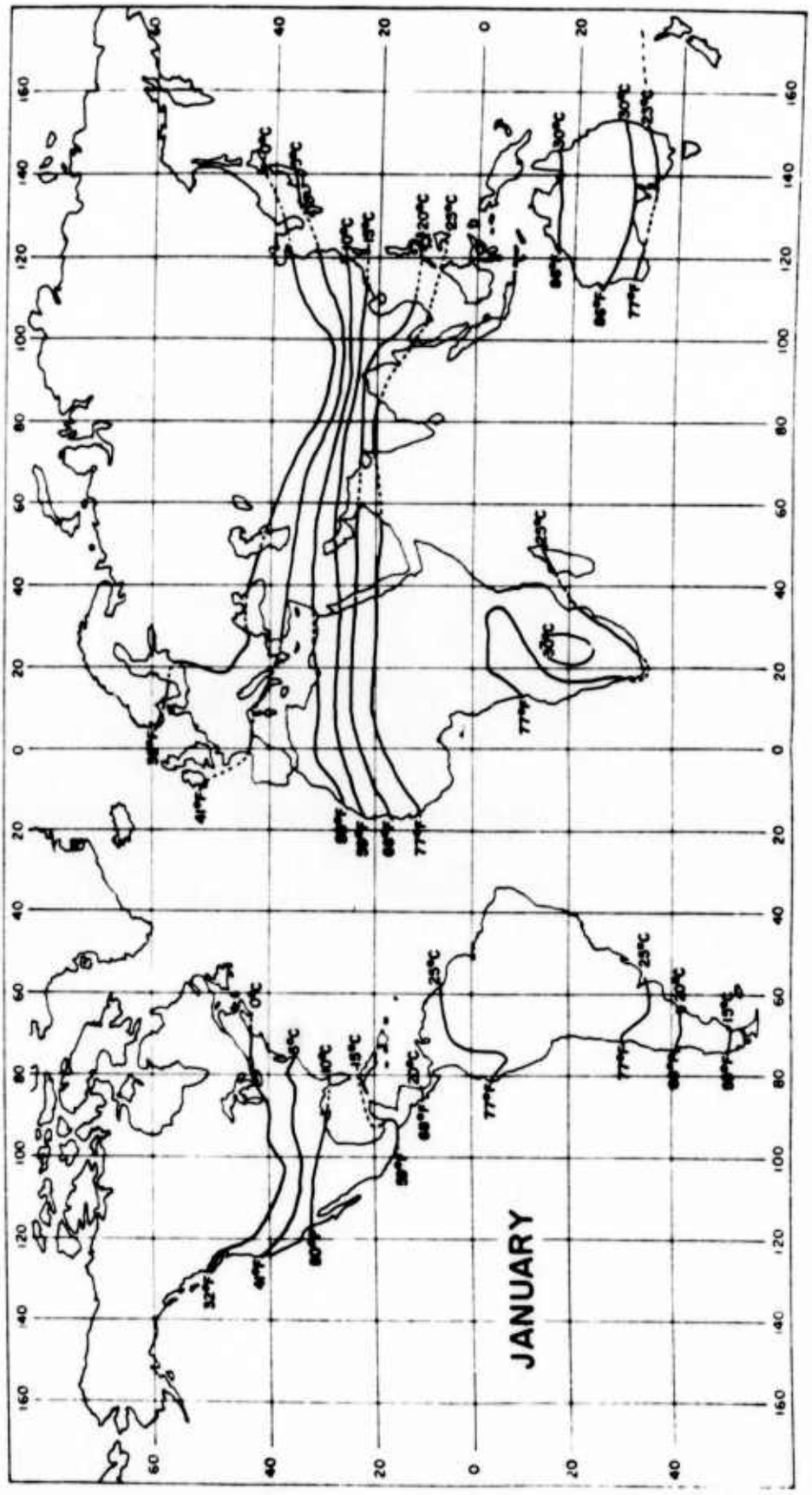


Fig. 14 — Soil temperature at 10-cm depth — January (Chang, 1958)

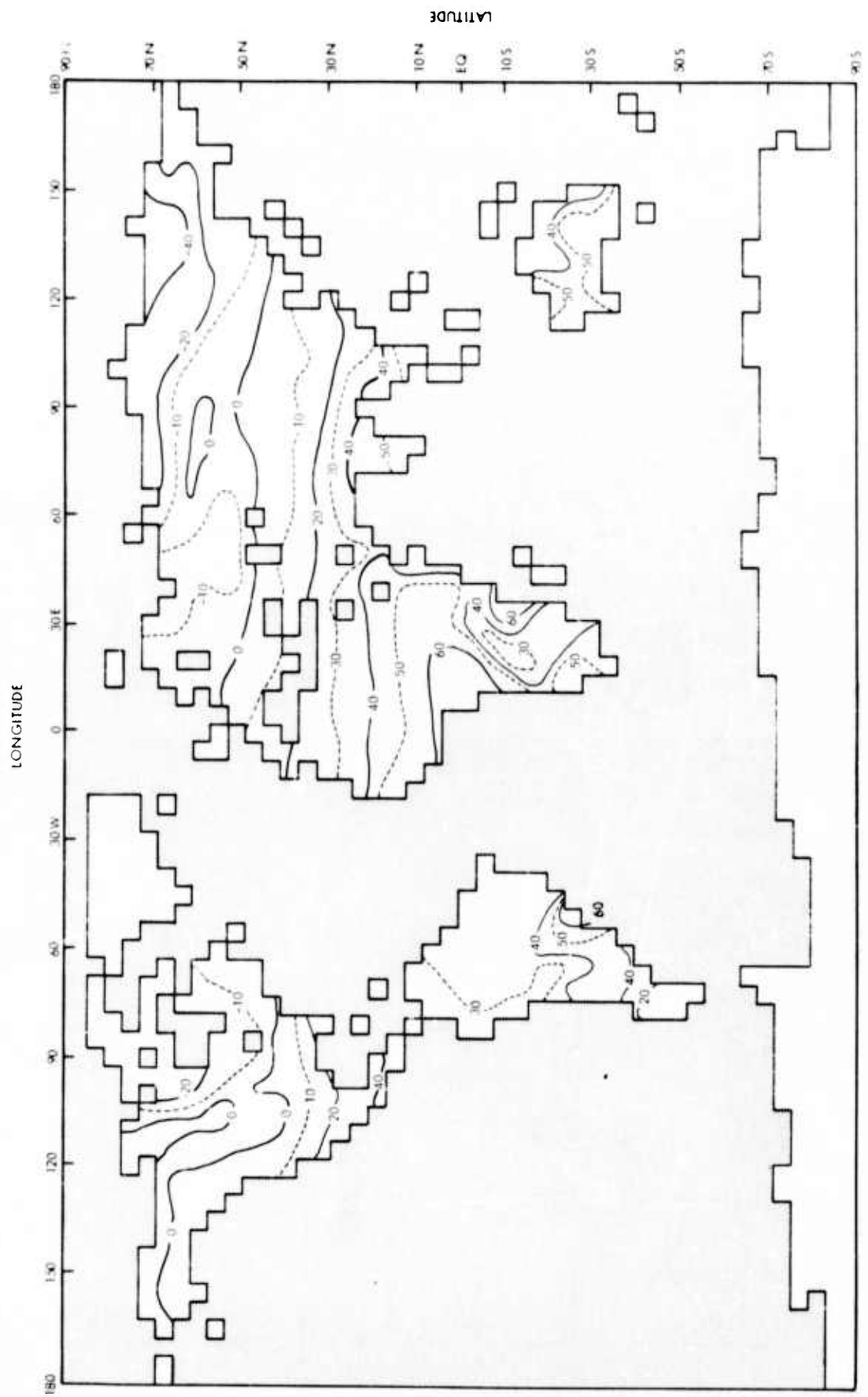


Fig. 15 — Daily maximum ground surface temperature (°C) - Experiment 4 (January)

January climate by Gates (1972) has shown this region to be characterized by heavy precipitation and consequently a high evaporation rate. It can perhaps be stated that this unrealistic feature of relatively higher surface temperatures in the equatorial African region will disappear in any long-term integration of the model.

Figure 16 shows distribution of the diurnal range of ground temperature. Again the unrealistic features displayed by the control run (Fig 3) have improved considerably, especially in Australia, South Asia, South America, and Africa. Figure 17 shows a plot of $T_g$, G, and solar radiation S as a function of local time. It can be seen that there is a phase lag of about 3 hours between maximum G and maximum $T_g$, and a lag of about 1 hour between maximum S and maximum $T_g$. These features agree very well with observations (Sellers, 1965; Lettau, 1951), as well as analytical solutions of the heat conduction equation, and are produced by the interaction of various components of the energy balance at the surface.

Experiment 5

Recently some atmospheric circulation models have computed the ground surface temperature ($T_g$) by solving an explicit prediction equation for $T_g$. According to Corby et al. (1972), the ground surface temperature can be computed from the equation

$$c \frac{\partial T_g}{\partial t} = S - R - H - LE \qquad (15)$$

where c is the heat capacity per unit area of the surface layer, and where S, R, H and LE have the same meaning as in the control and other experiments. It may be noted that Eq. (15) does not incorporate soil heat flux G explicitly. Consequently, we are not able to reproduce the diurnal variation of the surface temperature ($T_g$) realistically. In this experiment we describe our attempt to incorporate soil heat flux G in Eq. (15).

As shown by Sellers (1965), for example, in the absence of horizontal temperature gradients, the rate at which a soil layer is warming

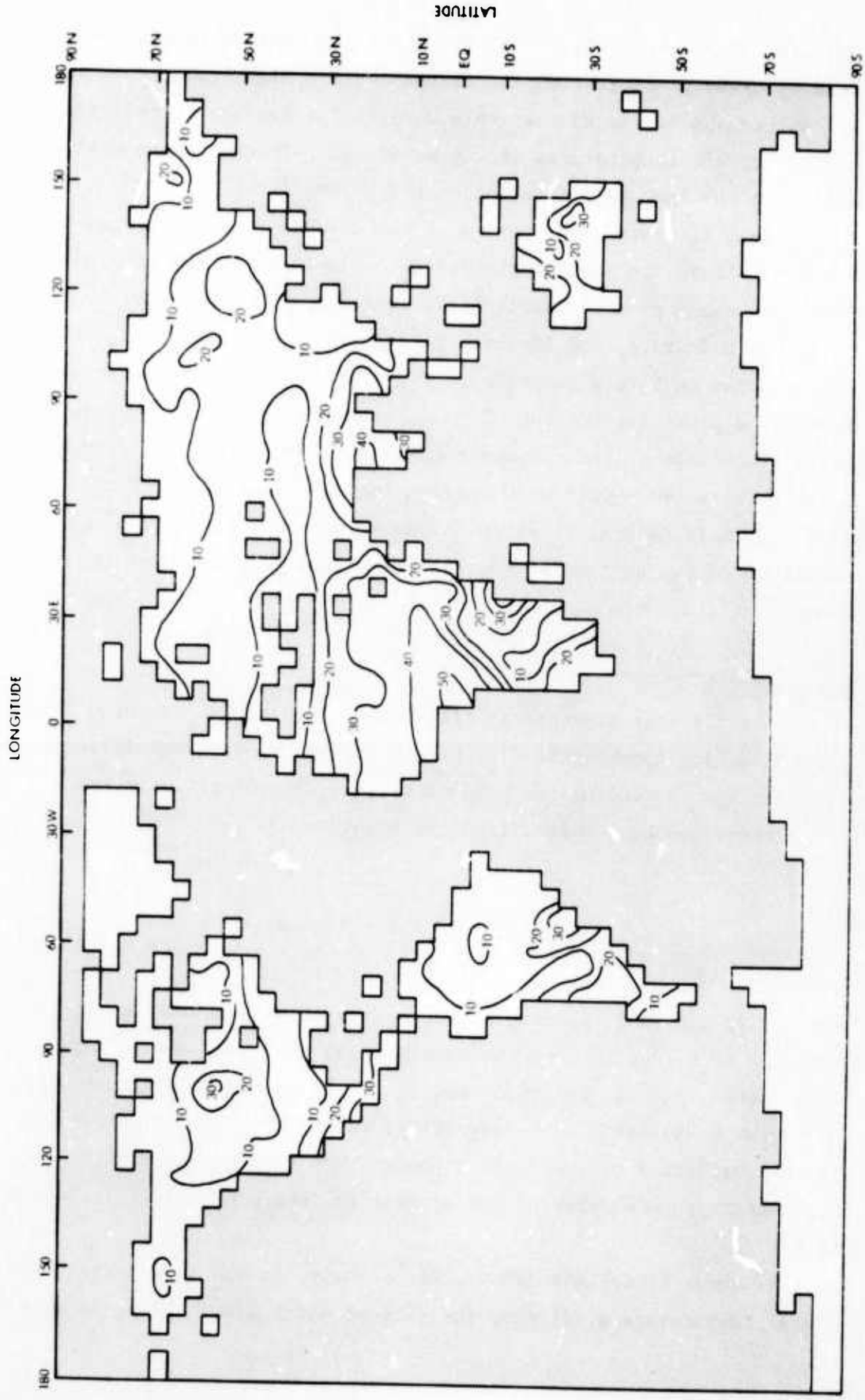


Fig. 16 — Diurnal range of ground surface temperature (°C) - Experiment 4 (January)

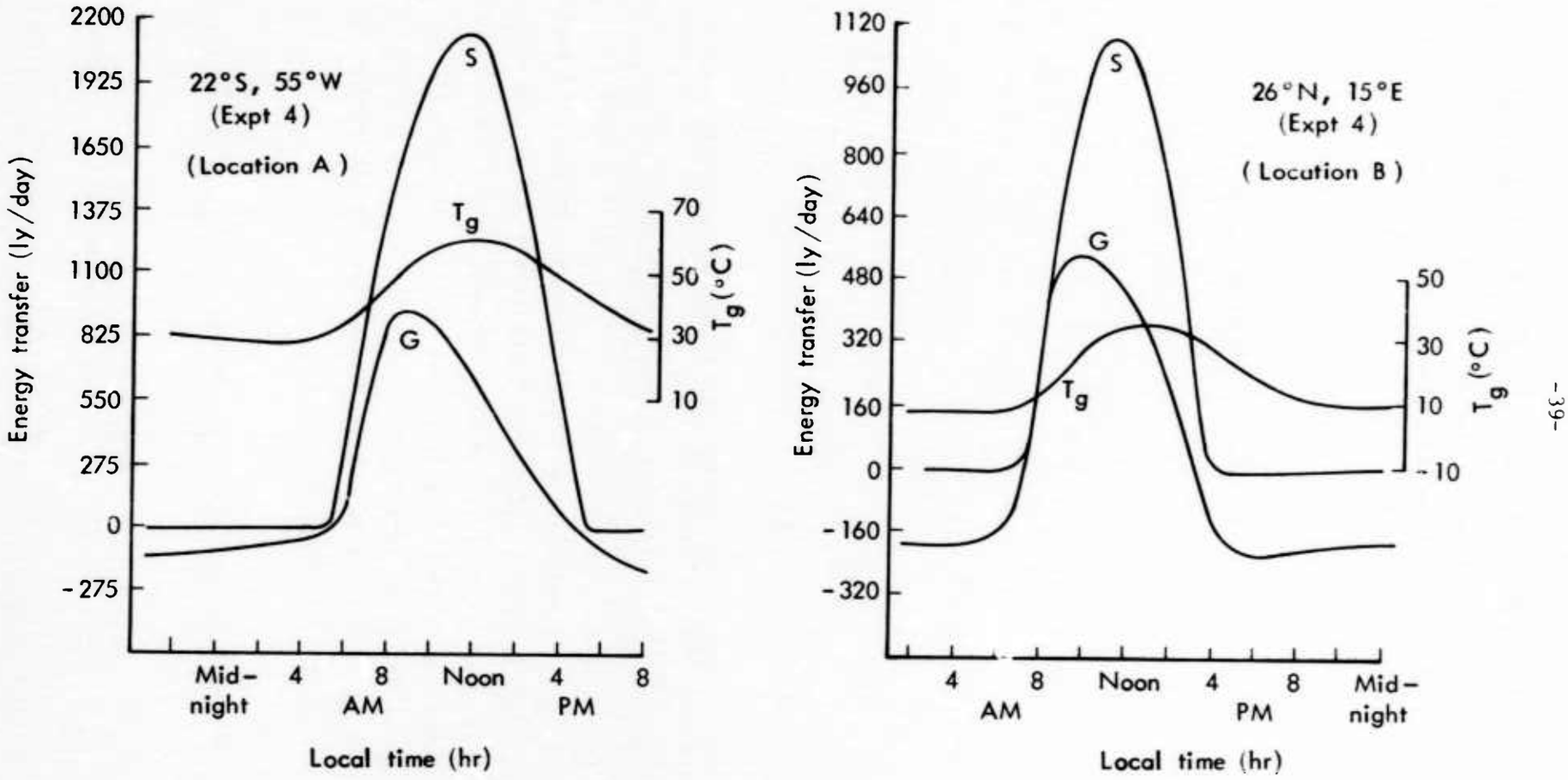


Fig.17 — Daily ground temperature ($T_g$ °C) and solar radiation (S, ly/day) as a function of local time at two selected locations for the month of January
(Expt 4)

or cooling is proportional to the net flux of energy into or out of the layer. Thus for a layer of thickness $\Delta z$ the observed time rate of temperature change is given by

$$-c \frac{\Delta T_g}{\Delta t} \Delta z = \Delta G$$

or, in differential form

$$c \frac{\partial T_s}{\partial t} = - \frac{\partial G}{\partial z} \tag{16}$$

Also, as shown in the Appendix, the soil heat flux G can be expressed as a function of z and t. Thus

$$G(z,t) = \Delta T_o \sqrt{\frac{\omega c \lambda}{2}} e^{-z/d} \left[ \sin \left( \omega t - \frac{z}{d} \right) + \cos \left( \omega t - \frac{z}{d} \right) \right] \tag{17}$$

or

$$G(z,t) = \sqrt{\frac{\omega c \lambda}{2}} \left[ \frac{1}{\omega} \frac{\partial T_s(z,t)}{\partial T} + T_s(z,t) - \bar{T} \right] \tag{18}$$

In practice it is preferable to use Eq. (18) rather than Eq. (17) because $\Delta T_o$, the amplitude of temperature wave at the soil surface, is rarely known (Sellers, 1965). De Vries (1963) and others have related $\Delta T_o$ to the amplitude of air temperature at 2 meters for the annual cycle, but such a relationship cannot be determined for the daily cycle because of the great variability involved.

Let us consider a soil layer extending from the surface (z = 0) to a depth z. Then by Eq. (16),

$$\left.\begin{array}{l} \longrightarrow \downarrow G(0) \longrightarrow (z = 0) \\ \\ \longrightarrow \downarrow G(z) \longrightarrow z \end{array}\right] \quad \begin{array}{l} c \dfrac{\partial T_s(z)}{\partial t} = - \left[ \dfrac{G(z) - G(0)}{z} \right] \\ \\ \text{or} \\ \\ cz \dfrac{\partial T_s(z)}{\partial t} = - [G(z) - G(0)] \end{array} \tag{19}$$

where $T_s(z)$ is the average soil temperature of layer of depth z

$G(0) \equiv$ S-R-H-LE is the soil heat flux at the surface $z = 0$ and involves ground temperature ($T_g$) of R, H, and LE, and dependence

$G(z)$, (Eq. (18)), is the soil heat flux at depth z.

However, since we were interested, mainly, in computing the ground surface temperature $T_g$, and also, since our model had no explicit levels within the soil, we used Eqs. (18) and (19) to obtain an equation that enabled us to predict $T_g$.

Let us consider a soil layer of 1-cm thickness. Since there is considerable uncertainty in defining "surface," particularly on global scale, and also because the horizontal grid size of our model is quite crude (4° latitude, 5° longitude), we can assume that average soil temperature for a layer of 1-cm depth approximates the ground surface temperature itself. Thus

$$T_s(1) \doteq T_g$$

Applying this approximation to Eqs. (18) and (19) at $z = 1$ cm, we obtain

$$G(1) \doteq \sqrt{\frac{\omega c \lambda}{2}} \left[ \frac{1}{\omega} \frac{\partial T_g}{\partial t} + T_g - \bar{T} \right]$$

and

$$c \frac{\partial T_g}{\partial t} = - [G(1) - G(0)] = G(0) - G(1)$$

Thus we have

$$c \frac{\partial T_g}{\partial t} = S - R - LE - H - \sqrt{\frac{\omega c \lambda}{2}} \left( \frac{1}{\omega} \frac{\partial T_g}{\partial t} + T_g - \bar{T} \right)$$

or, rearranging,

$$c_1 \frac{\partial T_g}{\partial t} = S - R - LE - H - \sqrt{\frac{\lambda c \omega}{2}} (T_g - \bar{T}) \qquad (20)$$

where

$$c_1 = \left(c + \sqrt{\frac{\lambda c}{2\omega}}\right)$$

It may be noted that, except for S, all terms on the right-hand side of Eq. (20) are functions of ground surface temperature $T_g$. Thus

$$c_1 \frac{\partial T_g}{\partial t} = F(T_g) \equiv S - R - LE - H - \sqrt{\frac{\lambda c \omega}{2}} (T_g - \bar{T})$$

Using the Newton-Raphston technique and appropriate formulations for R, LE, and H in $F(T_g)$ above,

$$T_g^{(t+1)} = T_g + \frac{S - R - H - LE - \sqrt{\frac{\lambda c \omega}{2}} (T_g - \bar{T})}{\frac{c_1}{\Delta t} + 4\nu T_g^3 + C_H\left(1 + \frac{L}{c_p} GW \frac{dq_s}{dT}\right) + \sqrt{\frac{\lambda c \omega}{2}}} \qquad (21)$$

Here $c_1 = c + \sqrt{\lambda c/2\omega}$ (c being volumetric heat capacity, prescribed as 0.6)

$\lambda$ = thermal conductivity (same as in Experiment 1)

$\bar{T}$ = average daily surface temperature, assumed same at all depths as prescribed in Experiment 4

$\omega$ = frequency of oscillation (same as in Experiment 4)

$\Delta t$ = time step of integration = 30 minutes (1/48 day)

$\nu$ = Stefan-Boltzmann constant = $1.171 \times 10^{-7}$ ly $day^{-1}$ $deg^{-4}$.

Other terms have the same meaning as in the earlier experiments of Sec. IV. The terms on the right-hand side are to be evaluated at time t.

We used Eq. (21) to predict ground surface temperature for a 48-hour period of January. Figures 18 and 19 show global distribution of daily maximum ground surface temperature and its diurnal range for January. A comparison of this with the control experiment shows a substantial decrease in the magnitude of the ground temperature. The results of Experiment 5 look similar to those of Experiment 4 (Fig. 15) except for the African continent, where the regions of high maximum surface temperature (>60°C) are much smaller in Experiment 5 than in Experiment 4. As regards diurnal range (Fig. 19), the amplitudes are smaller by 10° than those shown by Experiment 4 (Fig. 16) in the equatorial African region. The phase relationships between $T_g$, S, and G (not shown) are the same as those demonstrated in Experiment 4: the maximum in $T_g$ follows the maximum in solar radiation (S) by about an hour and follows, by about 3 hours, the maximum in soil heat flux G.

Even though results of Experiments 4 and 5 appear to be similar, it may be noted that Experiment 5 uses an *explicit* prediction equation for $T_g$, whereas in Experiment 4 it is implicit in the formulation of G. It may also be remarked that whereas the formulation of Experiment 4 is applicable *only* at the surface, that of Experiment 5 is more general and can be used to predict the temperature of a soil layer of finite depth and consisting of multiple levels.

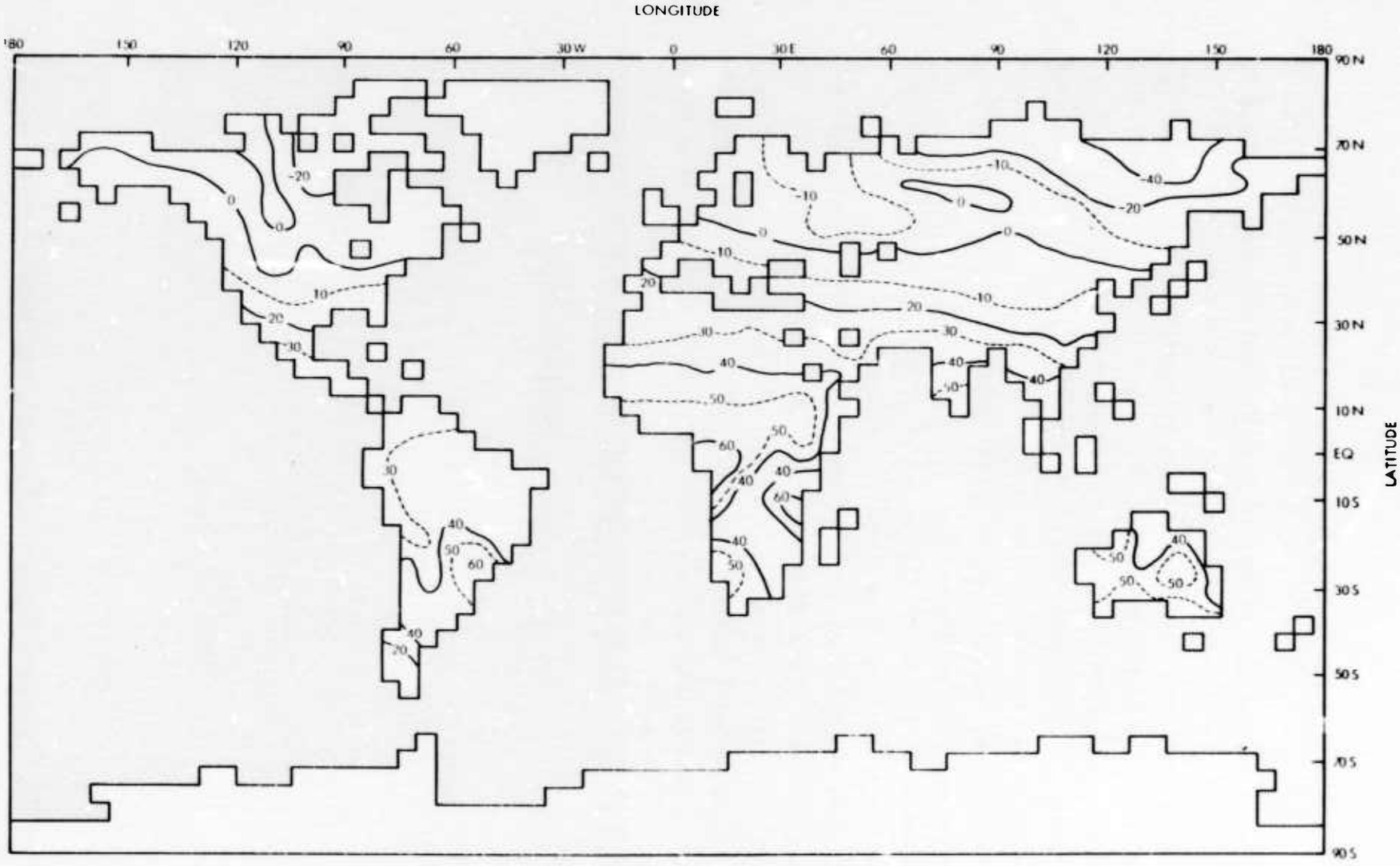


Fig. 18 — Daily maximum ground surface temperature (°C) - Experiment 5 (January)

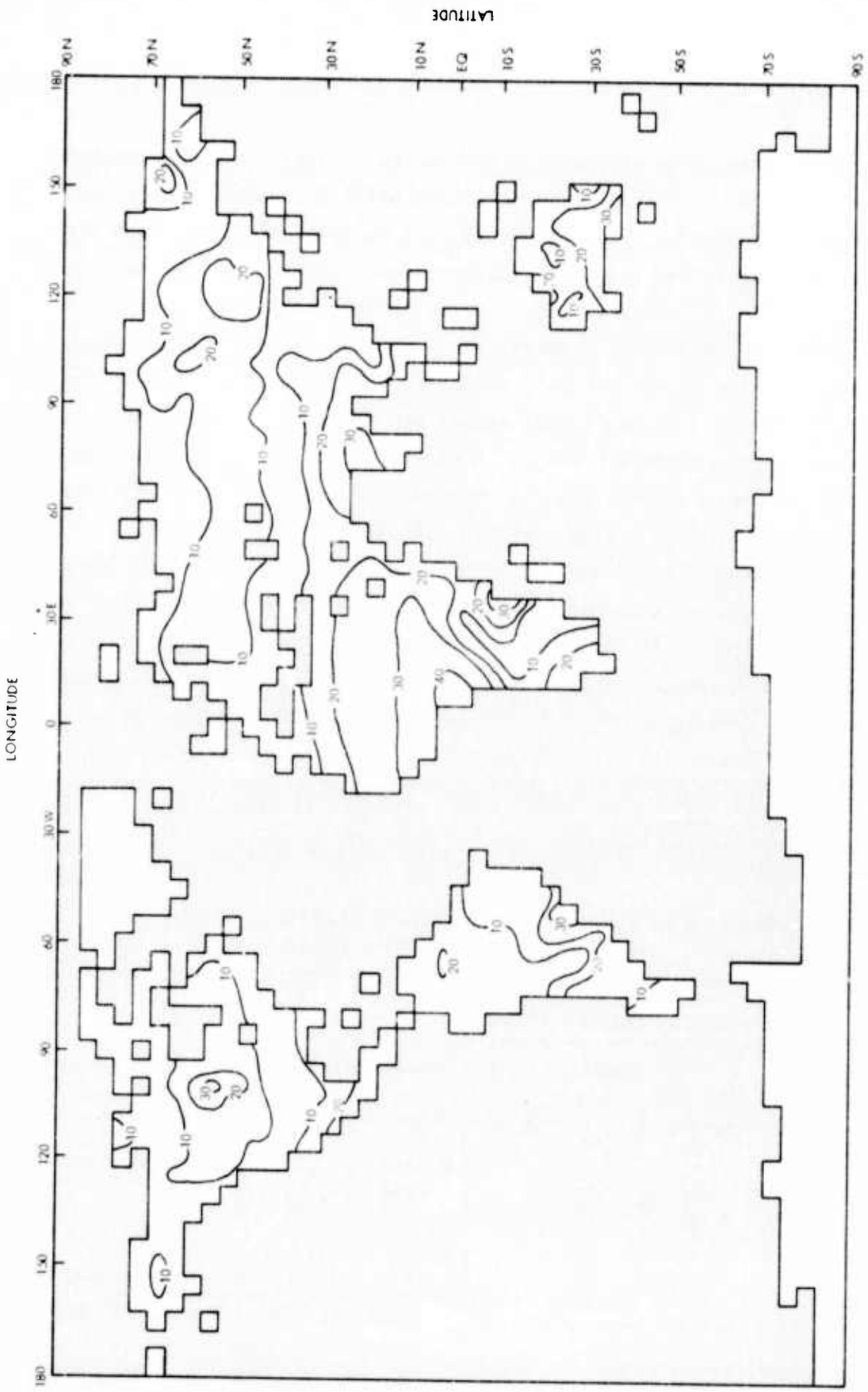


Fig. 19 — Diurnal range of ground surface temperature (°C) - Experiment 5 (January)

## VI. SUMMARY AND CONCLUDING REMARKS

In accordance with the purpose of this study, we have integrated the Rand two-level general circulation model to compute the ground (bare land) surface temperature ($T_g$) by incorporating soil heat flux in the heat balance equation (Experiments 1 through 3). We have also computed $T_g$ by taking into consideration the heat capacity of the soil as well as soil heat flux (Experiments 4 and 5). A comparison of results (Table 5) shows that the most realistic distribution of $T_g$ with respect to the magnitude, the diurnal range, and the phase relationships is obtained in Experiments 4 and 5. However, since the formulation for Experiment 5 is more general and can be used to compute the surface temperature of a soil layer of finite depth, it should be preferred to that of Experiment 4, especially if one can afford a model of multiple soil levels. The technique of Experiment 4 is considered adequate if only the interface temperature is required. Other methods such as the control experiment, Experiment 2 (Gadd and Keers, 1970), and Experiment 3 (Kasahara and Washington) are not realistic; the latter two involve extensive parameterization of the soil heat flux. This study has also demonstrated

Table 5

COMPARISON OF THE RESULTS OF VARIOUS NUMERICAL EXPERIMENTS AT LOCATION B (IN SAHARA REGION)

| Experiment | Ground Temperature (°C) | | Phase Relationship Between Maximum Values of $T_g$, S, and G |
|---|---|---|---|
| | Maximum | Diurnal Range | |
| Control | 40 | 46 | Maxima in $T_g$, S, G occur at same local time |
| 1 | 34 | 35 | |
| 2 | 39 | 38 | |
| 3 | 32 | 31 | |
| 4 | 31 | 28 | Maxima in Tg occur 1 hour after maxima in S and 3 hours after maxima in G |
| 5 | 27 | 22 | |

NOTE: $T_g$ is ground temperature, S is solar radiation, G is soil heat flux.

a good correspondence between the results of numerical experiments and the classic analytical solutions.

We have not considered the temperature of surfaces other than bare land. In order to simulate natural conditions we should also consider surfaces which may be covered with ice and/or snow. However, the atmospheric model used in this study prescribes a cover of ice and/or snow which does not change with time. Therefore we have not modified Eq. (1) for computing ground temperatures of surfaces other than bare land. Modifications of these conditions are currently in progress. Besides the nature of the cover on the surface, we should also consider its other properties such as texture, moisture content, organic matter, color, structure, cultivation, and topography.

The results described in this study are based on only a 48-hour integration of the basic circulation model. Consequently the conclusions cannot be generalized for long-term integration results.

Since we have integrated a basic circulation model for different experiments after varying *only* the formulations for soil heat flux, this study presents a valid comparison of the usefulness of different methods. It is felt that the techniques discussed can also be used in integrating local atmospheric and soil boundary layer models.

In recent times, considerable attention has been paid to the study of climatic changes and their impact on worldwide economic and social order. Though modeling of climatic variation is still in developing stages, general circulation models are being used increasingly to study shorter period variations. And recognizing the importance of feedback effects of variations of surface temperature on atmospheric processes, it is essential to be able to compute, among other things, a realistic distribution of ground surface temperature. The technique recommended in this report can be useful in this computation.

Appendix

AN EXPRESSION FOR HEAT FLUX INTO THE SOIL

Assuming that soil is homogeneous and that heat flow is in the vertical direction only, the heat conduction equation can be written as

$$\frac{\partial T_s}{\partial t} = \frac{\lambda}{c} \frac{\partial^2 T_s}{\partial z^2} \qquad \text{(A-1)}$$

where $T_s$ is soil temperature, $\lambda$ is thermal conductivity, and c is volumetric heat capacity.

Let us assume that at all depths z the temperature varies as a pure harmonic function around an average value. Though crude, this assumption enables us to approximate the description of actual fluctuations caused by the succession of day and night (diurnal) or winter and summer (seasonal). However, this must be modified for natural soil temperatures. Let us now assume that the temperature at the surface can be written as

$$T_s(0,t) = \bar{T} + \Delta T_o \sin(\omega t) \qquad \text{(A-2)}$$

where $\bar{T}$ is *daily* average temperature of the soil assumed to be the *same* at all depths, $\Delta T_o$ is the amplitude at the surface, and $\omega$ is frequency of oscillation and equals $2\lambda$/(period of the wave). Equation (A-2) is the boundary condition at $z = 0$. The solution of (A-1) may be written as

$$T_s(z,t) = \bar{T} + \Delta T_o e^{-z/d} [\sin(\omega t - z/d)] \qquad \text{(A-3)}$$

where $T_s(z,t)$ is the soil temperature at the depth z and time t and $d = \sqrt{2\lambda/c\omega}$ is the depth at which the amplitude of $\Delta T_o$ is insignificant.

Again, for an infinitesimally thin soil layer, the heat flux into the soil is given by

$$G(z,t) = -\lambda \frac{\partial T_s}{\partial z} \tag{A-4}$$

Combining (A-3) and (A-4), we get

$$G(z,t) = \Delta T_o \sqrt{\frac{\omega c \lambda}{2}}\, e^{-z/d} \left[\sin(\omega t - z/d) + \cos(\omega t - z/d)\right] \tag{A-5}$$

Also, from Eq. (A-3) we obtain

$$\Delta T_o e^{-z/d} \sin(\omega t - z/d) = T_s(z,t) - \bar{T}$$

and differentiating,

$$\Delta T_o e^{-z/d} \cos(\omega t - z/d) = \frac{1}{\omega} \frac{\partial T_s}{\partial t}$$

Therefore, by eliminating $\Delta T_o$, which is rarely known accurately, Eq. (A-5) can be written as

$$G(z,t) = \sqrt{\frac{\omega c \lambda}{2}} \left[\frac{1}{\omega} \frac{\partial T_s(z,t)}{\partial t} + T_s(z,t) - \bar{T}\right] \tag{A-6}$$

or at z = 0 (surface)

$$G(0,t) = \sqrt{\frac{\omega c \lambda}{2}} \left[\frac{1}{\omega} \frac{\partial T_g}{\partial t} + T_g - \bar{T}\right] \tag{A-7}$$

where $T_g = T_s(0,t)$ is the temperature at the surface.

## REFERENCES


Arakawa, A., *Design of the UCLA General Circulation Model*, Technical Report No. 7, Department of Meteorology, University of California, Los Angeles, July 1972.

Brooks, F. A., and W. B. Goddard, *Observed Four-Component Hourly Energy Balance*, Final Report, University of California, Davis, 1966.

Brunt, D., *Physical and Dynamical Meteorology*, Cambridge University Press, 1934.

Chang, Jen-Hu, *Ground Temperature*, Vol. I, Blue Hill Meteorological Observatory, Harvard University, Milton, Mass., June 1958.

Corby, G. A., A. Gilchrist, and R. L. Newson, "A General Circulation Model for the Atmosphere Suitable for Long Term Integrations," *Quart. J. Roy. Meteorol. Soc.*, Vol. 98, 1972, pp. 809-832.

Delsol, F., K. Miyakoda, and R. H. Clark, "Parameterized Processes in the Surface Boundary Layer of an Atmospheric Circulation Model," *Quart. J. Roy. Meteorol. Soc.*, Vol. 97, 1971, pp. 181-208.

de Vries, D. A., "Thermal Properties of Soils," in *Physics of Plant Environment*, edited by W. R. Van Wijk, John Wiley & Sons, Inc., New York, 1963.

Eckert, E., and R. Drake, Jr., *Heat and Mass Transfer*, McGraw-Hill, New York, 1959.

Estoque, M. A., "A Numerical Model of the Atmospheric Boundary Layer," *J. Geophys. Res.*, Vol. 68, No. 4, February 1963, pp. 1103-1113.

Gadd, A. J., and J. F. Keers, "Surface Exchanges of Sensible and Latent Heat in a 10-Level Model Atmosphere," *Quart. J. Roy. Meteorol. Soc.*, Vol. 96, 1970, pp. 297-308.

Gates, W. L., *The January Global Climate Simulated by the Two-Level Mintz-Arakawa Model: A Comparison with Observation*, The Rand Corporation, R-1005-ARPA, November 1972.

Gates, W. L., E. S. Batten, A. B. Kahle, and A. B. Nelson, *A Documentation of the Mintz-Arakawa Two-Level Atmospheric General Circulation Model*, The Rand Corporation, R-877-ARPA, December 1971.

Geiger, R., *The Climate Near the Ground*, Harvard University Press, Cambridge, Mass., 1965.

Ingersoll, L., O. Zobel, and A. Ingersoll, *Heat Conduction*, McGraw-Hill, New York, 1948.

Jacobs, C. A., and P. S. Brown, Jr., "An Investigation of the Numerical Properties of the Surface Heat Balance," *J. Appl. Met.*, Vol. 12, No. 6, September 1973, pp. 1069-1072.

Johnson, J. C., *Physical Meteorology*, The M.I.T. Press, Cambridge, Mass., 1954.

Johnson, N. K., and E. L. Davies, "Some Measurements of Temperature Near the Surface in the Various Kinds of Soils," *Quart. J. Roy. Meteorol. Soc.*, Vol. 53, 1927, pp. 45-59.

Kasahara, A., and W. Washington, "General Circulation Experiments with a Six-Layer NCAR Model, Including Orography, Cloudiness and Surface Temperature Calculations," *J. Atm. Sci.*, Vol. 28, No. 5, July 1971, pp. 657-701.

Lettau, H., "Theory of Surface-Temperature and Heat-Transfer Oscillations Near a Level Ground Surface," *Transactions, American Geophysical Union*, Vol. 32, No. 2, April 1951, pp. 189-200.

Lonnquist, O., "On the Diurnal Variation of Surface Temperature," *Tellus*, Vol. 14, No. 1, February 1962, pp. 96-101.

Lonnquist, O., "Further Aspects on the Diurnal Temperature Variation at the Surface of the Earth," *Tellus*, Vol. 15, No. 1, February 1963, pp. 75-81.

Manabe, S., J. Smagorinsky, and R. F. Strickler, "Simulated Climatology of a General Circulation Model with a Hydrologic Cycle," *Monthly Weather Review*, Vol. 93, No. 12, December 1965, pp. 769-798.

Myrup, L. O., "A Numerical Model of the Urban Heat Islands," *J. Appl. Met.*, Vol. 8, No. 6, December 1969, pp. 908-918.

Outcalt, S. I., "The Development and Application of a Simple Digital Surface-Climate Simulator," *J. Appl. Met.*, Vol. 11, No. 4, June 1972, pp. 629-636.

Pandolfo, J. P., D. S. Cooley, and M. A. Atwater, *The Development of a Numerical Prediction Model for the Planetary Boundary Layer*, Final Report, The Travelers Research Center, Inc., Hartford, Conn., 1965.

Priestley, C.H.B., *Turbulent Transfer in Lower Atmosphere*, The University of Chicago Press, Chicago, 1959.

Sasamori, T., "A Numerical Study of Atmospheric and Soil Boundary Layers," *J. Atm. Sci.*, Vol. 27, No. 8, November 1970, pp. 1122-1137.

Sinclair, J. G., "Temperatures of the Soil and Air in a Desert," *Monthly Weather Review*, Vol. 50, 1922, pp. 142-144.

Sellers, W. D., *Physical Climatology*, The University of Chicago Press, Chicago, 1965.

Sutton, O., *Micrometeorology*, McGraw-Hill, New York, 1953.